Hydrochemistry of the shallow alluvial and regional sandstone aquifers in the semi-arid River Goulbi de Maradi Basin of Niger

Boukari Issoufou Ousmane[1] · Yahaya Nazoumou[1] · Guillaume Favreau[2] · Maman Sani Abdou Babaye[3] · Rabilou Abdou Mahaman[1] · Marie Boucher[1,2] · James P.R. Sorensen[4] · Alan M. MacDonald[5] · Richard Graham Taylor[6]

[1]Département de Géologie, Faculté des Sciences et Techniques, Université Abdou Moumouni, Niamey, Niger

[2]Institut de Recherche pour le Développement, Niamey, Niger, CNRS, Grenoble INP, IGE, France

[3]Département de Géologie, Faculté des Sciences et Techniques, UMR SERMUG, Université Dan Dicko Dan Koulodo, Maradi, Niger

[4]British Geological Survey, Maclean Building, Wallingford, OX10 8BB, United Kingdom of Great Britain and Northern Ireland UK

[5]British Geological Survey, Lyell Centre, Research Avenue South, Edinburgh EH14 4AP, United Kingdom of Great Britain and Northern Ireland UK

[6]Department of Geography, University College London, London WC1E 6BT, United Kingdom of Great Britain and Northern Ireland UK

Abstract

In the River Goulbi de Maradi Basin (RGMB), groundwater is a vital source of drinking water and plays a central role in the region's socio-economic development through irrigation. The quality of these groundwater resources and their suitability for irrigation and drinking-water supplies remain inadequately understood. Here we compare the results of hydrochemical analyses of 23 samples from the shallow (screen intake depth <30 m below ground level) alluvial (9) and underlying deeper (>40 m below ground level) Continental Hamadien (CH) sandstone aquifer (14) against standard measures for the suitability of groundwater for drinking water (World Health Organization (WHO) guideline values) and irrigation (i.e. sodium adsorption ratio, sodium percentage, and the residual sodium carbonate). All sampled groundwater from the alluvial aquifer was suitable for irrigation compared to 65% (9/14) of the groundwater samples from the CH. Fluoride concentrations exceeding the WHO drinking-water guideline value of 1.5 mg/L were recorded in 1 sample from the alluvial aquifer and 3 samples from the CH aquifer. Hydrochemical facies reveal most samples are Na-HCO_3, Na-HCO_3, and Na-Cl types in the alluvial and CH aquifers. Bivariate plots combined

with saturation indices and electrical conductivity monitoring indicated that the main hydrogeochemical processes influencing the water are water-rock interactions, controlled by soil leaching during the surface runoff and the river infiltration in the unsaturated zone for the alluvial aquifer; cation exchange is dominant processes into CH aquifer. Our results highlight the general suitability of groundwater for drinking water supplies and irrigation in the RGMB and address a paucity of data on groundwater quality in the Sahel.

Keywords hydrochemistry · groundwater · water-rock interactions · Sahelian zone

Introduction

Groundwater is a vital source of fresh water in many parts of Sub-Saharan Africa (MacDonald et al. 2012). From rural areas to big cities, there remains tremendous dependence on groundwater either solely or in conjunction with surface water to meet water needs for drinking water, livestock rearing, industry, and irrigation (Nazoumou et al. 2016; Cobbing and Hiller 2019). Due to the rapid growth of population and urbanization (UN 2019), and for the achievement of the UN Sustainable Development Goals (SDGs 2 and 6), groundwater withdrawals are expected to increase substantially (Gaye and Tindimugaya 2019; Cobbing 2020) to address rapid increases in demand for domestic water supplies (Adams et al. 2018) and irrigation for food security (Altchenko and Villholth 2015; Nazoumou et al. 2016). Additionally, due to its high and underexploited potential in some regions and its resilience to climate variability and change (Cuthbert et al. 2019; Taylor et al. 2022), groundwater discharges play a fundamental role in maintaining and restoring ecosystems (Carter and Parker 2009; Taylor et al. 2013).

In the Sahelian drylands, rainfall is highly variable in space and time (Lebel and Ali 2009). As a result, surface water resources are unreliable and often ephemeral, insufficient to sustain sharply rising demand due to increasing populations and socio-economic development (Mahe et al. 2005; Descroix et al. 2009). Groundwater is consistently the only perennial source of freshwater throughout the year (Favreau et al. 2009, 2012; Abdou Babaye et al. 2019, 2021), supporting poverty alleviation (Favreau et al. 2009, 2012; Nazoumou et al. 2016) and adaptation to climate variability and change associated with increased intensity and severity of droughts and floods (Tschakert et al. 2010; Taylor et al. 2013; Elagib et al. 2021). Despite the fundamental role played by groundwater in supporting socio-economic development, and ecosystem function, data on

groundwater systems are sparse and the current state of knowledge is limited (MacDonald et al. 2012; Xu et al. 2019).

In the Sahel, groundwater quantification and the process of its renewal have been the focus of water resources assessments. Substantial groundwater volumes are considered to be stored in regional sedimentary aquifers (Favreau et al. 2012) and several recent studies have sought to resolve the processes that govern groundwater recharge (Favreau et al. 2009; Abdou Babaye et al. 2019; Cuthbert et al. 2019; Goni et al. 2021). An increase in surface runoff has been observed in response to the modification of soil properties and infiltration capacities caused by the clearing of perennial grasses (Leblanc et al. 2008; Mahe et al. 2013). This land-cover change has led to sharp increases in surface runoffs amplifying river flow and the size and number of ponds (Descroix et al. 2009, 2012). Widespread connectivity of surface water to aquifers is the dominant process in groundwater replenishment, even during drought years (Favreau et al. 2009). Notwithstanding the indispensable role that groundwater plays in the drylands of the Sahel, there is a paucity of data on their suitability for different uses and the hydrogeochemical processes controlling these.

Groundwater is perceived as a safe and reliable source of water for drinking. As a consequence, less attention is paid to water quality analyses, restricting understanding and ability to manage and protect groundwater sources (Lapworth et al. 2022). However, there is a need to focus greater attention towards groundwater quality because there is a direct connection between stores of available fresh-water provided by groundwater and their status and utility in terms of quality (Gleeson et al. 2020). Groundwater is vulnerable to natural and anthropogenic contamination (Lapworth et al. 2012, 2017; Onipe et al. 2020). Due to significant pressures from anthropogenic activities and climate variability, the protection of groundwater resources is necessary for sustaining human health, groundwater-dependent livelihoods, and ecosystems (Lapworth et al. 2022). Inadequate management of anthropogenic waste contributes to chemical and organic contamination of groundwater, posing health risks to hundreds of millions of people (WHO 2019) and livestock raising. Natural processes associated with local geology can affect groundwater quality, through water/rock interactions which often lead to ion exchange or weathering/dissolution of certain minerals in groundwater (Abdou Babaye et al. 2019; Zhao et al. 2021).

In the River Goulbi de Maradi Basin (RGMB), surface waters are limited in time and space. The basin's water supply and irrigation are ensured exclusively by groundwater within a shallow Quaternary alluvial aquifer largely constrained to the river's floodplain and an underlying regional Upper Cretaceous sandstone aquifer known as the Continental Hamadien (CH). Due to the growth of urban and rural populations, freshwater demand has increased rapidly (WHO/UNICEF 2015). In addition, according to the national policy of Niger (MHA 2016), a multi-village water supply requiring intensive groundwater pumping is planned to increase the drinking-water supplies in pursuit of UN Sustainable Development Goal (SDG) 6 (water and sanitation for all). Intensive pumping is proposed from deep boreholes, screened in the lower part of the CH aquifer that is thought to be replenished by the overlying alluvial aquifer (Issoufou Ousmane et al., 2022). Water quality assessments in this region are, however, few. Recently, high fluoride concentrations exceeding guideline values of WHO (2011) have been observed by the Ministry of Hydraulics and Sanitation and led to the closure of many dug wells and boreholes. In International Federation for Human Rights report (FIDH 2002), it was reported that approximately more than 500 and 4500 cases of skeletal and dental fluorosis, respectively, in children aged under 15 years old, following the consumption of water pumped from deep boreholes. Assessment of groundwater quality for human health and irrigation, as well as the determination of their mineralization processes, is necessary to promote groundwater safety and improve integrated groundwater management.

The objectives of this study are: (1) to study the distribution of hydrochemical characteristics of alluvial and Continental Hamadien aquifer, and (2) to determine the processes governing groundwater mineralization, including high fluoride concentration. The results of this study are intended to serve as an aid for authorities in the planning and management of groundwater, in particular for the drinking-water supply and irrigation.

Study area

The RGMB is located in the south-central of the Sahel of southeastern Niger and northern Nigeria within the southeastern edge of the Iullemmeden sedimentary basin (Fig. 1a and b). It's bounded to the east and north by the Goulbi Kabba fossil valley and, to the west by the Goulbi Bounsourou valley (Fig. 1c). This region is one of the most densely populated in Niger with between 81 and 105 inhabitants/km^2. The River Goulbi de Maradi is the only source of surface water. The river is seasonal, flowing episodically from July to October depending on local rainfall and releases from

119 the Jibya dam in Nigeria (storage capacity: 142 million m^3). The climate is semi-arid, featuring a
120 single rainy season (June to early October), controlled by the monsoon (hot and humid). A long
121 dry season occurs from November to May (Fig. 2a) governed by the harmattan (dry and very hot)
122 coming from the Sahara desert (Issa Lélé and Lamb 2010). Mean (1960 to 2017) annual rainfall is
123 520 mm (Fig. 2b). Mean monthly temperatures and real evapotranspiration range from 25 to 35°C
124 and 150 to 210 mm, respectively (Fig. 2a).

125 The geological context consists of Quaternary formations, the Continental Hamadien (CH)
126 of the Upper Cretaceous, and the crystalline to crystallophyllian Precambrian basement. The
127 Quaternary is characterized by alluvium encountered in the valley with a thickness varying from 0
128 to 30 m, and aeolian deposits formed on the plateaux comprising reddish sand with subordinate
129 clay, 5 to 10 m thick at maximum (BRGM 1978; Durand et al. 1981; Issoufou Ousmane et al.
130 2021). The Continental Hamadien (CH) is made up in the study area of continental deposits, which
131 represent the lateral equivalent of the marine deposit formed in the Upper Cretaceous (Dikouma
132 1990; Greigert 1966). In the RGMB, in particular, analyses of lithological logs of wells and
133 boreholes reveal that CH is composed of pebbly sand series upstream, clays sandstone series
134 downstream, and Farak-type sandstones localized at the base of the ensemble (Issoufou Ousmane
135 et al., 2022) (Fig. 3). The Precambrian basement, which consists of granites, gneisses, and schists
136 of Paleoproterozoic to Cambrian age, is exposed in the southern part of the study area along the
137 Nigerian border in an east-west direction. It is in geological continuity with the northern Nigerian
138 shield mobile zone (Mignon 1970).

139 Hydrogeologically, the alluvial aquifer has a depth varying from 4 to 18 m, respectively, in
140 the upstream and downstream part of the GM basin. The aquifer extends laterally across the valley
141 by 1.5 to 4 km and is used mainly for irrigation and population water supply. Conversely, the CH
142 aquifer is located on a regional scale, between Niger, Nigeria, Benin, and Mali (OSS 2008).
143 According to (Issoufou Ousmane et al., 2022), the alluvial and CH aquifer are in hydraulic
144 continuity.

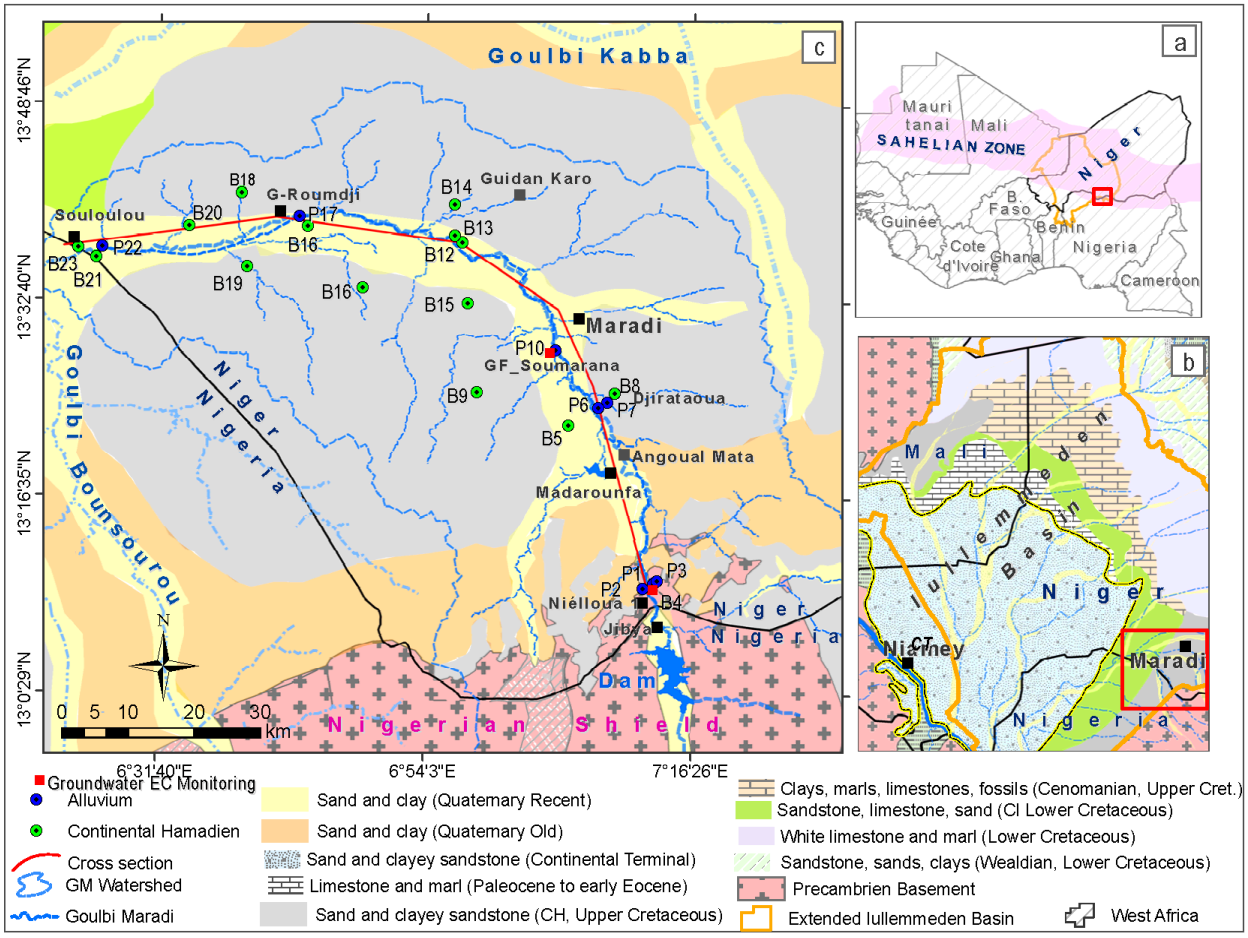

Fig. 1 Map location: **a** Map of West Africa showing the location of the Sahelian zone, Iullemmeden basin and study area; **b** geological map of the Iullemmeden Basin; **c** map of the River Goulbi de Maradi Basin

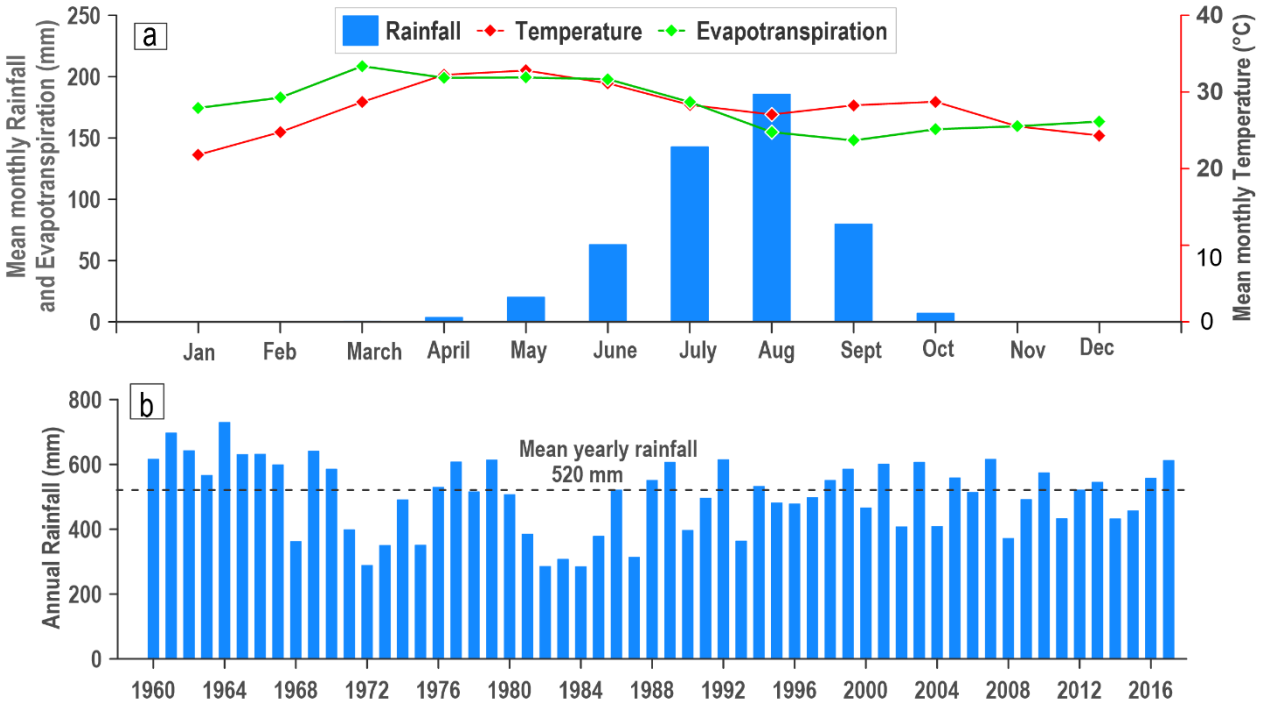

149

150 **Fig. 2** Climatic parameters in the study area at the Maradi airport synoptic station: **a** monthly data
151 for rainfall (from 1960-2017), temperature (from 1950-2017) and real evapotranspiration (from
152 1984-2010); **b** annual rainfall (from 1960 to 2017), all data were provided by the Direction de la
153 Météorologie Nationale (DMN)

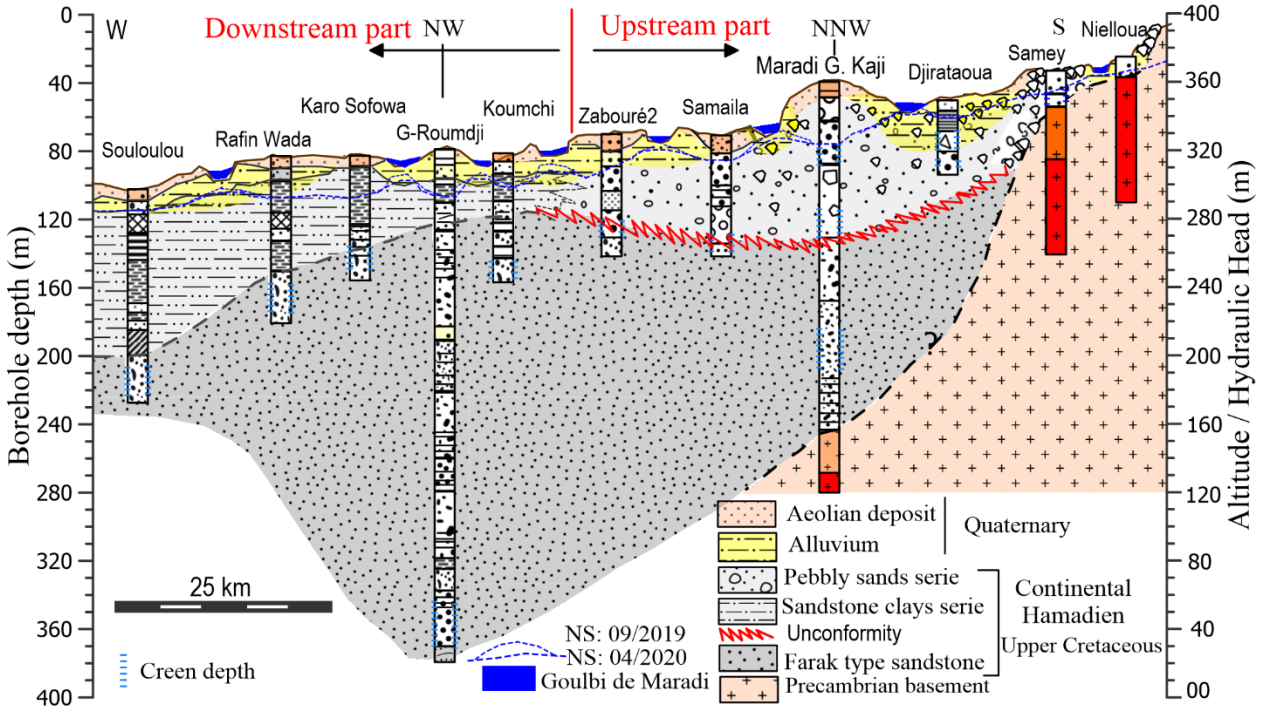

154

Fig. 3 Upstream-downstream hydrogeological section along the River Goulbi de Maradi as shown in Figure 1 (Issoufou Ousmane et al., 2022).

Material and methods

Sampling and analytical methods

In this study, 23 samples comprising 9 observation wells (piezometers) within the alluvial aquifer and 14 boreholes used for drinking-water supplies from the regional sandstone aquifer of the Continental Hamadien (CH) were collected in November 2018 (Fig. 1a). Boreholes screened in the CH aquifer were selected from an existing database with details of total depth drilled, screen depth, and water-table depth (Table 1). In this way, groundwater from the CH aquifer was specifically sampled from boreholes whose total depth drilled exceeded 60 m with screen intake depths below 40 m in depth. In the alluvial aquifer, piezometers constructed to depths from 6 to 30 m under this research were sampled. For data presentation, each source has been assigned a code (P = piezometer in the Quaternary alluvium and B= borehole in the CH) (Table 1; Fig. 1a). Prior to sampling, boreholes were pumped with 12V submersible WaSP P5 pump (In-Situ Europe Ltd, UK) for 30 minutes to 2 hours to remove three (3) times the volume of the stored water in the borehole. This volume is obtained by the difference between the total depth and borehole static water level according to the diameter.

Physico-chemical parameters, measured in situ after stabilization, include pH, redox potential (E_h), and dissolved oxygen (DO), and their probes were installed in a flow-through cell sealed from the atmosphere. Probes measuring specific electrical conductivity (EC) and temperature (T) were conducted in an overflowing beaker. Measurements of EC, pH, DO, and E_h were carried out using Seven2GoTM pro meters (Mettler Toledo, Switzerland) and temperature using a HI-93510 thermistor thermometer (Hanna® instruments, USA). In addition, to avoid equipment drifts and minimize measurement errors, calibration was done daily. Samples for major ions (cations and anions) analysis were taken in 30 ml Nalgene bottles. Before sampling, the bottles were washed three times with distilled water and water from the boreholes and then filtered using a 0.45 µm cellulose nitrate membrane. Samples were stored in a cooler to prevent exposure to excessive heat variations.

Sample analysis for anions (Cl^-, SO_4^{2-}, F^-, NO_3^-, and NO_2^-) were carried out by ion chromatography using the Dionex system (AS50, Thermo Fisher Scientific, USA) at UKCEH, Wallingford, UK. Major cations Ca^{2+}, Mg^{2+}, Na^+, K^+, SiO_2, and trace elements Ag, As, Ba, Cu, Fe, Mn, Ni, Pb, Rb, Sr, U, and Zn concentrations were measured with Inductively Coupled Plasma Mass Spectrometry (ICP-MS-QQQ Agilent 8900) (Agilent Technologies, USA) at BGS Keyworth, UK. The detection limits range from 2, 0.7 and 0.003 mg/L for Ca^{2+}, Na^+ and K^+ and for Mg^{2+} ions, respectively. For trace elements, the detection limits are between 0.2 and 0.002 µg/L.

Table 1 Characteristics of wells sampled. P= Piezometer, B= Borehole, n.a= not available

Site Code	Date	Lat (°)	Long (°)	SWL (m)	Borehole Depth (m)	Screen Depth (m)
Alluvial aquifer						
P1	13/11/2018	13.15838	7.21516	4.22	06	6.5 - 10.5
P2	12/11/2018	13.15756	7.21214	4.93	12	8.5 - 11
P3	12/11/2018	13.15898	7.21720	5.25	13	n.a
B4	12/11/2018	13.15763	7.21233	4.96	n.a	n.a
P6	07/11/2018	13.39977	7.13799	9.25	15	5.2 - 14
P7	17/11/2018	13.40051	7.14204	11.26	19	9.6 - 12.6
P10	09/11/2018	13.47871	7.08163	5.17	11	n.a
P17	13/11/2018	13.65916	6.72276	17.76	33	23 - 29
P22	08/11/2018	13.61607	6.44799	12.47	25	18 - 24
Continental Hamadien aquifer						
B5	09/11/2018	13.37566	7.10104	14.43	76	37 - 55
B8	16/11/2018	13.41985	7.16488	44.16	83	49 - 61
B9	08/11/2018	13.42048	6.97296	47.45	88	61 - 82
B11	14/11/2018	13.54182	6.95861	27.94	63	51 - 60
B12	15/11/2018	13.62467	6.95102	14.0	90	49 - 70
B13	15/11/2018	13.63459	6.94024	14.82	62	44 - 47
B14	15/11/2018	13.67661	6.94021	30.91	64	49 - 61
B15	13/11/2018	13.56260	6.81250	51.38	91	76 - 88
B16	14/11/2018	13.64616	6.73495	30.62	70	58 - 67
B18	11/11/2018	13.69146	6.64175	40.6	83	66 - 90
B19	10/11/2018	13.59005	6.65027	26.89	61	44 - 58
B20	10/11/2018	13.64548	6.56951	26.14	95	73 - 93
B21	08/11/2018	13.60222	6.43945	19.62	87	65 - 80
B23	08/11/2018	13.61513	6.41468	23.78	145	105 -135

Chemical data analysis tools

Analyses sought to assess the suitability of waters for human consumption and irrigation and identify geochemical processes controlling the acquisition of water mineralization. In this sense, the analytical results were compared to World Health Organization standards (WHO 2011). Cations Ca^{2+}, Mg^{2+}, (Na^{+} + K^{+}) and the anions HCO_3^{-}, SO_4^{2-} and (Cl^{-} + NO_3^{-}), were represented on the diagram of Piper (1944) for identifying the chemical facies of the water. Diagrams of Gibbs (1970), which are constructed by plotting the ratio of $Na^{+}/(Na^{+} + Ca^{2+})$ and $Cl^{-}/(Cl^{-} + HCO_3^{-})$ versus TDS, were implemented to explore natural processes governing groundwater geochemistry such as atmospheric precipitation, rock-water interaction, and evaporation (Li et al. 2016; Su et al. 2019). To identify ion sources, bivariate diagrams, chloro-alkaline indices 1 and 2 (CAI-1 and CAI-2) proposed by Schoeller (1965), and the diagram [(Na^{+} + K^{+}) - Cl^{-}] versus [(Ca^{2+} + Mg^{2+}) - (HCO_3^{-} + SO_4^{2-})] (Fisher and Mullican III 1997) were developed based on the ionic ratios. The CAI-1 and CAI-2 were used to demonstrate cation exchange between groundwater and the host rock. Based on Schoeller (1965), exchange between Na^{+} or K^{+} into the groundwater with Ca^{2+} or Mg^{2+} of the host rock is identified when the values of the CAI-1 and 2 are positive. While, when Ca^{2+} or Mg^{2+} from groundwater exchange for Na^{+} or K^{+} from the host rock, both indices are negative (Chidambaram et al. 2013; Li et al. 2016).

Schoeller indices are calculated using the formulas of Schoeller (1965), where all ions are expressed in meq/L:

$$\mathrm{CAI}-1=\frac{\mathrm{Cl}^{-}-(\mathrm{Na}^{+}+\mathrm{K}^{+})}{\mathrm{Cl}^{-}} \quad (1)$$

$$\mathrm{CAI}-2=\frac{\mathrm{Cl}^{-}-(\mathrm{Na}^{+}+\mathrm{K}^{+})}{\mathrm{HCO}_3^{-}+\mathrm{SO}_4^{2-}+\mathrm{CO}_3^{2-}+\mathrm{NO}_3^{-}} \quad (2)$$

The theory of Fisher and Mullican (1997) is based on the principle that while cation exchange is an important process affecting the chemical composition of water, the scatter plot of the diagram [(Na^{+} + K^{+}) - Cl^{-}] versus [(Ca^{2+} + Mg^{2+}) - (HCO_3^{-} + SO_4^{2-})] follows along the line of slope -1 (Li et al. 2019; Su et al. 2019). In the same way, to examine the potential for dissolution or precipitation of halite, gypsum, calcite, dolomite, and fluorite, the saturation indices (SI) of these minerals were calculated using the geochemical speciation model PHREEQC (Parkhurst and Appelo 2013). SI < 0, indicates undersaturation, so the mineral should dissolve if present, SI > 0, indicates supersaturation, so the mineral should precipitate, and SI = 0, indicates saturation.

Since the chemical composition of irrigation water can affect both agricultural yield and soil properties, it is critical to assess the quality of irrigation water. The following indicators were employed: sodium adsorption rate (SAR), the percentage of soluble sodium (%Na), and residual sodium carbonate (RSC). The (%Na) and the SAR are valuable parameters in the evaluation process of groundwater suitability for irrigation because they provide a basis for determining sodium alkalinity hazard in irrigation water as they directly relate to the absorption of sodium on the soil surface (Davraz and Özdemir 2014; Li et al. 2016; Zaman et al. 2018). Water characterized by a high %Na and SAR can produce an accumulation of sodium in the soil, which can lead to a decrease in macroporosity and the rate of water infiltration. The suitability of irrigation water is also determined by the Wilcox diagram quality (Wilcox 1948), using the relationship between percent sodium (%Na) and electrical conductivity (EC). According to this classification, irrigated water is classified into four categories: good to permissible, permissible to doubtful, doubtful to unsuitable, and unsuitable. While residual sodium carbonate (RSC) indicates the deleterious effect of carbonate (CO_3^{2-}) and bicarbonate (HCO_3^-) on the quality of water for agricultural use (Eaton 1950). If the RSC < 1.25, water is safe for irrigation, and if it exceeds 2.5, the water is considered unsuitable (Ramesh and Elango 2012).

These parameters are expressed by the following relationships; where cations and anions are in meq/L.

$$\mathrm{SAR} = \frac{\mathrm{Na^+}}{\sqrt{\frac{\mathrm{Ca^{2+}+Mg^{2+}}}{2}}} \qquad \text{(eq. 3)}$$

$$\%\,\mathrm{Na} = \frac{\mathrm{Na^+}}{\mathrm{Ca^{2+}+Mg^{2+}+Na^+ + K^+}} \times 100 \qquad \text{(eq. 4)}$$

$$\mathrm{RSC} = (\mathrm{CO_3^{2-}} + \mathrm{HCO_3^-}) - (\mathrm{Ca^{2+}} + \mathrm{Mg^{2+}}) \qquad \text{(eq. 5)}$$

Groundwater and surface water monitoring

To better understand the relationship between surface water and groundwater, as well as their seasonal dynamics, high frequency (hourly) monitoring of groundwater levels (GWL) and electrical conductivity (EC), was implemented in 4 piezometers, namely Nielloua1, Nielloua_GF01, Soumarana1, and GF_Soumarna, all screened in the alluvial aquifer. GWL and EC monitoring was undertaken at Niélloua1 and Soumarana1 by the Maradi Regional Direction of

Hydraulics and Sanitation (DRH/A-Maradi) respectively from May 2015 and September 2016 to December 2020, using CTD-Diver dataloggers (Van Essen Instruments). While at Nielloua_GF01 and GF_Soumarana, GWL and EC were monitored using dataloggers Aqua TROLL 200 and Level TROLL 500 (In-Situ Inc.) from June 2017 to April 2020 under the GroFuture research project. The river's stage height has been measured manually at Niélloua, through readings on a stream-gauging station, twice a day, in the morning and the evening. To better study surface and groundwater dynamics, groundwater levels and river stage were converted to hydraulic head, using topographic leveling data made relative to sea level datum.

Results

Hydrochemistry and drinking water quality assessment

Physico-chemical parameters of water

Physicochemical characteristics of sampled groundwater in the alluvial and CH aquifers were analyzed statistically and compared to the WHO (2011) standards to provide the general characteristics of the water in the RGMB. Table 2 presents the maximum (Max), minimum (Min), mean, median, and standard deviation from each variable. The water temperature varies from 29.3 to 31.1°C in the alluvial aquifer and 30.7 to 33.8°C in the CH. The average values are 30.1-31.9°C, and the standard deviations are 0.5-0.7°C, respectively. Groundwater is mostly acidic, with pH values ranging between 5.46 and 6.99 in the alluvium and 5.27 and 7.26 pH units in the CH, except for one sample in which the value of 8.91 was obtained. The average values are 6.30 and 6.49 for standard deviations of 0.49 and 0.92, respectively.

Electrical conductivity (EC) presents highly variable values ranging from 78-550 µS/cm in alluvium and 66-2030 µS/cm in CH. The average values are 270 and 500 µS/cm. Regarding alluvium, relatively high values between 200 and 550 µS/cm were measured in the irrigated perimeters. While, in the underlying CH aquifer, high electrical conductivity values ranging from 900 to 2000 µS/cm were measured in boreholes located in the downstream part, where the equipped depths exceeded 60 meters. The dissolved oxygen (DO) contents range from 0.1 to 2.7 mg/L in the alluvial aquifer and 0.1 to 3.1 mg/L in the CH aquifer. The average values are 0.8 and 1.2, and the standard deviations are 0.8 and 1.5 respectively for alluvium and CH. Water redox potential (Eh) values vary from -136 to +185 mV in the alluvial aquifer and from -170 to +250 mV in the CH.

277 The average values and the coefficients of variation are respectively 43 and 105 mV, and 288 and
278 119%. Relative to the guidelines (WHO 2011), observed physicochemical parameters in sampled
279 groundwater (Table 2) suggest that it was suitable for human consumption, except for a single
280 sample (F13) presenting a conductivity of 2030 µS/cm.

281 **Table 2** Statistical analysis of physico-chemical parameters of groundwater samples in alluvium
282 and CH aquifers

variable	N	Max	Min	Average	Median	Stand. Deviation	(OMS, 2011)
Alluvial aquifer							
T (°C)	9	31.1	29.3	30.1	30.2	0.5	
Eh (mV)	9	185	-137	43	69	125	
pH	9	6.99	5.46	6.30	6.32	0.49	6.5–8.5
DO (mg/l)	9	2.7	0.1	0.8	0.3	0.9	na
EC (µS/cm)	9	556	78	271	227	163	1000
Continental Hamadien aquifer							
T (°C)	14	33.8	30.7	31.9	31.9	0.8	
Eh (mV)	14	251	-171	106	130	126	
pH	14	8.91	5.27	6.49	6.37	0.92	6.5–8.5
DO (mg/l)	14	3.1	0.1	1.2	0.6	1.5	na
EC (µS/cm)	14	2031	67	507	233	560	1000

283 na: not available

284 **Chemical parameters and groundwater type**

285 Major-ion and trace-element compositions of groundwater (Table 3) are plotted in Fig. 4 and show
286 wide variabilities between the two aquifers. Based on their major-ion concentrations, each
287 groundwater sample was assigned a hydrochemical facies (Fig. 5). Groundwater sampled from the
288 shallow alluvial aquifer belongs to the hydrochemical facies Na-HCO_3 and Ca-HCO_3, respectively,
289 for 6 and 3 samples (n=9) with concentrations of Na^+ (6.5-83 mg/L), Ca^{2+} (6-33 mg/L) and HCO_3^-
290 (31.3-288 mg/L). For the underlying CH sandstone aquifers, four (4) facies were determined,
291 namely the Na-HCO_3, Na-Cl, Ca-HCO_3, and Ca-Cl respectively to 6, 4, 2, and 2 samples (n=14)
292 with concentrations of Na^+ (31.3-288 mg/L), Ca^{2+} (<2-85 mg/L), Mg^{2+} (<0.003-8 mg/L), HCO_3^-
293 (23.4-255 mg/L) and Cl^- (1.11-394.9 mg/L). However, the Na-Cl facies was particularly
294 determined for water sampled in the downstream part of the RGMB. It should be noted both in the
295 alluvial and CH aquifer the Na^+ and HCO_3^- ions are dominant; the composition generally shows
296 the following decreasing order: $Na^+ > Ca^{2+} > K^+ > Mg^{2+}$, $HCO_3^- > Cl^- > SO_4^{2-} > NO_3^- > F^-$ for
297 cations and anions, respectively. For the long-term evolution of hydrochemical facies, based on

298 chemical analyses performed in 1960 (Greigert 1963), the facies Na-HCO_3 were dominant in both
299 the alluvium and the CH.

300 To assess the risk to human health posed by groundwater as a drinking water, major-ion and
301 trace-element concentrations were compared with the drinking-water quality standards
302 recommended by WHO (2011) (Fig. 4). Major-ion concentrations in both aquifers were
303 consistently below tolerance thresholds values, except a sample (B13) from the CH aquifer located
304 downstream (Fig. 1c), in which concentrations of Na^+ (397 mg/L) and Cl^- (395 mg/L) exceeded
305 WHO guideline values. Though the relative elevated concentration of these ions in groundwater
306 may not pose any adverse health risk to consumers, high concentrations (> 250 mg/L) of sodium
307 ions and chloride in water might interact to form sodium chloride, which could confer a salty taste
308 to the water (WHO 2011). High fluoride concentrations in the alluvial aquifer were measured in a
309 single sample 2.2 mg/L at P3, Fig. 1c). This sample is located in the upstream part of the RGMB
310 around the Niger-Nigerian border where the thin alluvium is in contact with the weakly altered
311 granitic basement rock (Fig. 1c). In the CH aquifer, high concentrations of fluoride exceeding the
312 guideline value were measured in boreholes of drinking water supply located downstream (Fig. 1c)
313 at B12 (4.3 mg/L), B13 (3.5 mg/L), and B20 (3.0 mg/L) at depths respectively of 90, 62, and 95 m.

314 Except for boron (B) absent in the alluvial aquifer, trace elements (Si, Ba, Sr, Mn, Fe, OxFe,
315 Li, Al, Cr, Co, Ni, Cu, Zn, Rb, Mo, Ag, Cd, Pb, U), were detected in more than 80% of the samples
316 in the two aquifers. The low B content below the detection limit (<93µg/L) in the alluvial aquifer
317 is likely associated with lower concentrations in the lithology of the alluvium. For most trace
318 elements (Ag, Ba, Cu, Sr, Fe, As, Mn, Ni, Pb, Rb, U, Zn) reported in Fig. 4, measured
319 concentrations were far below drinking-water guideline values (WHO 2011). However, Mn
320 concentrations exceeded guideline value of 0.1 mg/L (WHO 2011) at B4, P6, P7 and P10 with
321 recorded values of 0.99, 0.32, 0.47, and 0.29 mg/L. According to Mechal et al. (2022),
322 overconsumption of Mn beyond the acceptable limit may result in infertility, malfunction of the
323 immune system, and Parkinson-like symptoms.

324

325 Table 3 Major-ion and trace element compositions of the alluvial and Continental Hamadien aquifer. ng: not given; nm: not mentioned

	Major Ions (mg/L)									Traces Elements µg/L											
	Ca^{2+}	Mg^{2+}	Na^{+}	K^{+}	HCO_3^{-}	SO_4^{2-}	Cl^{-}	F^{-}	NO_3^{-}	Ag	Ba	Cu	Sr	Fe	As	Mn	Ni	Pb	Rb	Sio_2	U	Zn
WHO*	75	50	200	12	ng	250	250	1.5	50	ng	1300	2000	nm	ng	10	400	70	10	nm	nn	30	ng
Alluvial Aquifer																						
P1	33	6.29	83.0	2.70	167	17.9	65.14	0.38	50.27	0.5	256	1.6	305	63.2	1.45	21	0.51	0.05	1.2	45.3	0.872	05
P2	12	2.49	9.40	2.50	57.1	1.48	6.41	0.29	06.45	0.4	148	0.3	124	325	1.61	113	0.41	0.19	1.2	20.8	0.084	05
P3	33	6.11	38.9	50.1	288	2.95	5.40	2.17	00.06	0.3	259	0.6	221	781	0.84	101	0.33	0.13	9.2	74.7	19.8	03
F4	22	4.25	10.3	4.60	116	1.12	3.85	0.2	00.10	0.3	193	0.3	172	1350	10.0	985	0.36	0.08	1.8	38.0	0.232	05
P6	08	2.51	40.1	1.60	137	4.45	2.13	0.68	00.08	0.3	79.8	0.5	86.3	2871	2.90	320	1.48	1.31	1.5	37.9	0.956	20
P7	16	4.76	35.6	2.10	149	4.16	2.93	0.68	02.75	0.3	265	0.4	166	183.0	3.42	474	0.49	0.06	5.5	41.8	0.812	07
P10	13	3.97	23.9	6.50	104	8.87	7.76	0.43	01.96	0.3	113	1.1	155	1360	0.30	289	0.89	3.13	3.6	23.0	0.415	07
P17	11	2.89	7.60	4.30	45.5	5.27	1.97	0.17	20.82	0.3	294	0.5	179	22.20	0.08	8.20	0.40	0.39	9.8	21.3	0.149	05
P22	06	1.21	6.50	2.20	31.3	2.45	5.84	0.09	00.41	0.3	95.5	0.5	129	35.00	0.05	24.5	0.34	0.29	2.6	33.8	0.161	16
Average	**11**	**4**	**28**	**9**	**122**	**5**	**11**	**0.6**	**9**	**0.3**	**189**	**0.6**	**170**	**777**	**2**	**259**	**0.6**	**0.6**	**4**	**37**	**3**	**8**
Continental Hamadien Aquifer																						
B5	<2	<0.003	<0.7	<0.08	27.8	0.27	1.11	0.12	10.68	0.3	<0.1	<0.2	<0.2	<0.4	<0.04	<0.2	<0.06	<0.03	<0.3	<	<0.01	<0.8
B8	07	1.98	1.9	6.40	24.1	0.70	3.70	0.13	14.21	0.3	263	3.6	123	54.5	0.05	151	2.13	0.45	20.8	30.3	0.134	55
B9	07	1.73	2.5	6.60	42.3	0.12	0.59	0.18	03.0	0.3	233	0.9	138	1.20	<0.04	1.2	0.96	0.06	18.7	21.5	0.136	13
B11	11	3.37	5.8	7.90	23.4	9.20	24.81	0.07	6.85	0.4	416	1.3	183	21.7	<0.04	4.1	3.48	0.17	18.7	25.6	0.491	09
B12	04	0.63	190	2.70	167	79.26	154.5	4.32	2.34	0.3	24.6	0.5	160	56.8	0.34	2.6	0.19	0.11	07.0	20.7	0.218	02
B13	23	3.69	397	6.50	255	181.29	394.9	3.51	0.09	0.3	40.2	0.5	815	434	0.53	32.9	0.58	1.71	21.4	17.8	0.302	04
B14	29	8.13	149	8.70	127	67.68	196.2	0.41	2.44	0.4	75.2	0.7	632	9.90	0.05	0.6	1.05	0.14	29.4	22.9	1.43	04
B15	18	2.36	12.2	7.90	103	1.08	3.36	0.14	6.57	0.3	703	22.1	595	6.00	0.18	14.5	0.67	0.61	13.4	19.2	2.11	30
B16	06	1.56	7.40	3.90	47.6	1.48	2.08	0.07	5.48	0.3	222	3.7	169	30.5	0.08	1.8	0.48	0.63	16.1	26.1	0.275	06
B18	85	6.93	66.9	12.8	158	48.94	165.6	0.00	0.04	0.4	146	0.3	2218	73.4	<0.04	117	0.51	0.03	21.1	22.8	0.181	02
B19	07	2.31	19.4	4.40	65.3	2.81	6.99	0.14	5.23	0.3	242	1.3	101	9.70	<0.04	0.2	0.62	0.16	18	19.9	0.38	17
B20	04	1.59	2.70	4.30	195	81.51	120.3	3.01	1.38	0.3	170	0.7	67.4	5.40	0.06	1.8	0.54	0.08	13.8	28.6	0.256	15
B21	09	0.82	52.7	3.50	157	5.19	5.68	0.53	2.77	0.3	145	0.4	365	7.90	0.43	5.1	0.14	0.05	3.1	21.7	5.78	10
B23	<2	0.09	80.8	0.60	164	25.83	13.21	1.12	0.04	0.3	29.7	<0.2	73.1	2.70	1.84	0.3	<0.06	<0.03	0.6	15.1	0.01	01

Average	**17**	**3**	**76**	**6**	**111**	**36**	**78**	**0.98**	**4**	**0.3**	**208**	**3**	**434**	**59**	**0.4**	**25**	**0.9**	**0.4**	**16**	**23**	**0.9**	**13**

326

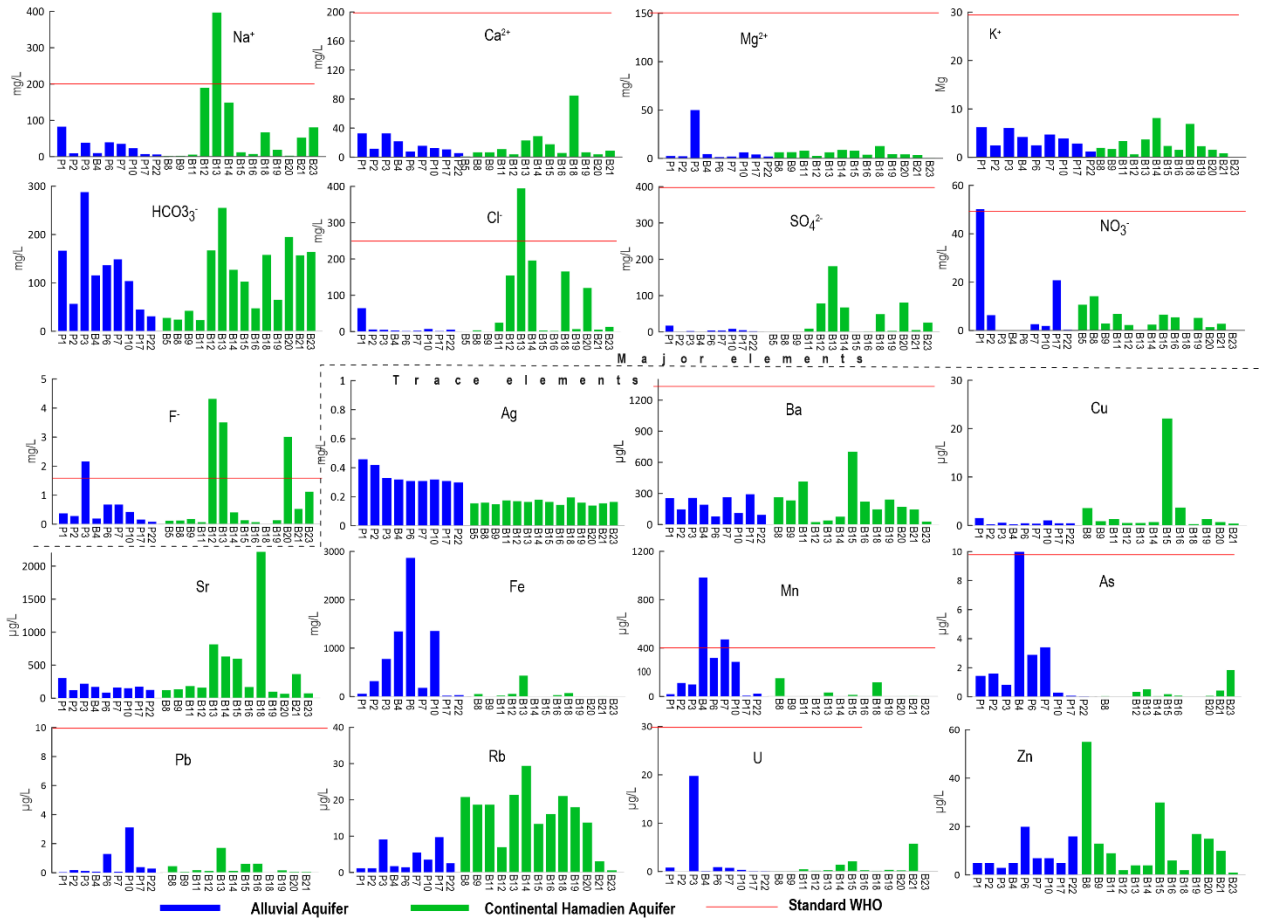

Fig. 4 Major ions and trace elements compositions of the alluvial and Continental Hamadien aquifer compared with WHO (2011) standard

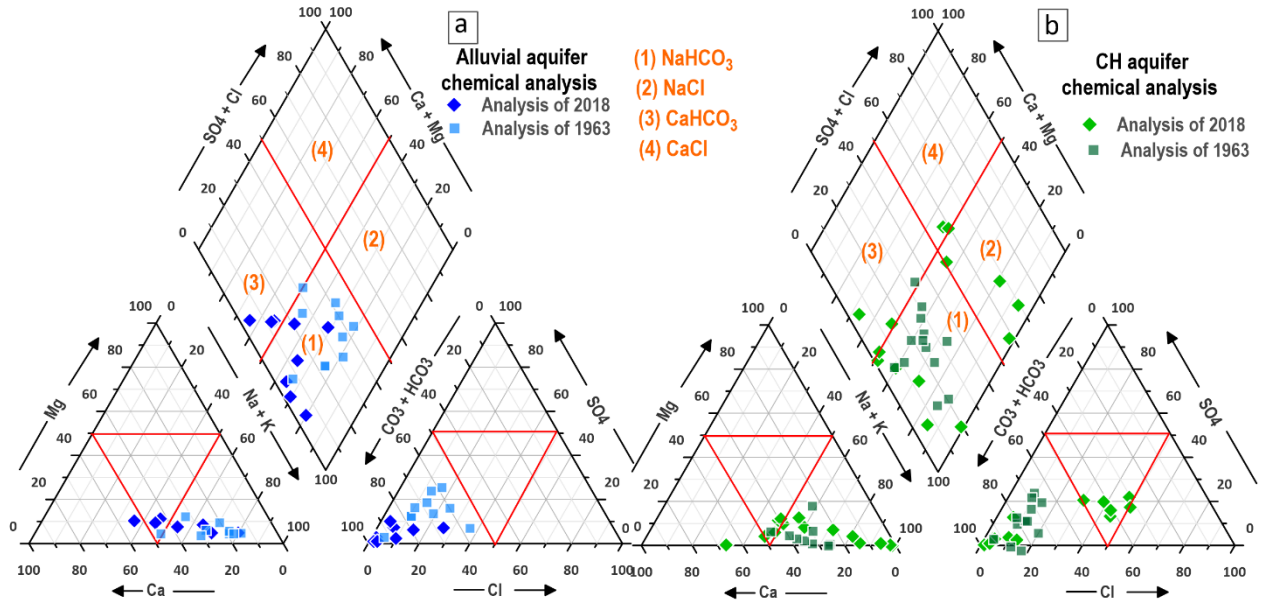

Fig. 5 Piper diagram showing hydrochemical facies of groundwater sampled from the alluvial and Continental Hamadien aquifers

Seasonal variation in groundwater level and electrical conductivity

Fig. 6 presents hourly hydraulic head and electrical conductivity of the alluvial aquifer and river stage at the Nielloua and Soumarana sites. At the Nielloua site, the depth of the water table is between 3-4 m, and the piezometers Nielloua_GF01 and Nielloua1 are located at 50 m and 270 m from the river, respectively. While at Soumarana, the piezometer Soumarana1 and Soumarana_GF01 are located at 50 m and 380 m from the river, and the depth of the water table is ranging from 4 to 6 m. The hydrographs show a seasonal variation of the piezometric level, with the maximum recorded around the end of September, which corresponds to the end of the river GM seasonal flows, while the minimum level is recorded around the end of May to the beginning of June. Relative hydraulic heads vary between 369-372 m at Nielloua_GF01, 368-370 m at Nielloua1 (Fig. 6a), 333-337 m at GF_Soumarana and 331.5-334 at Soumarana1 (Fig. 6b) and the corresponding fluctuation rates are 3, 2, 4 and 2.5 m, respectively. However, the most elevations of hydraulic heads are recorded in the Nielloua_GF01 and GF_Soumarana piezometers, located near the river, and the magnitude of this increase depends on the amplitude and duration of seasonal river flows, which also depends on the hydrological year. The hydraulic heads of the river ranging from 371-374 m and 339-342 m at Nielloua and Soumarana, respectively, are higher compared to

those of the piezometers in both sites, creating a hydraulic gradient towards the groundwater and driving focused recharge from the river GM flows infiltration.

Hourly monitoring of groundwater electrical conductivity shows that it varies from 80 to 160 µS/cm at Soumarana and from 160 to 200 µS/cm at Nielloua. It is noted that exceptional values of 280 µS/cm were measured at Nielloua in 2020 in response to increased river flow. Therefore, concomitantly with the seasonal increase in groundwater hydraulic head, a seasonal variation in electrical conductivity was measured for these sites, with an increase during the river flow stage period. This increase in conductivity suggests that mineralization is acquired through groundwater recharge by infiltration of river GM.

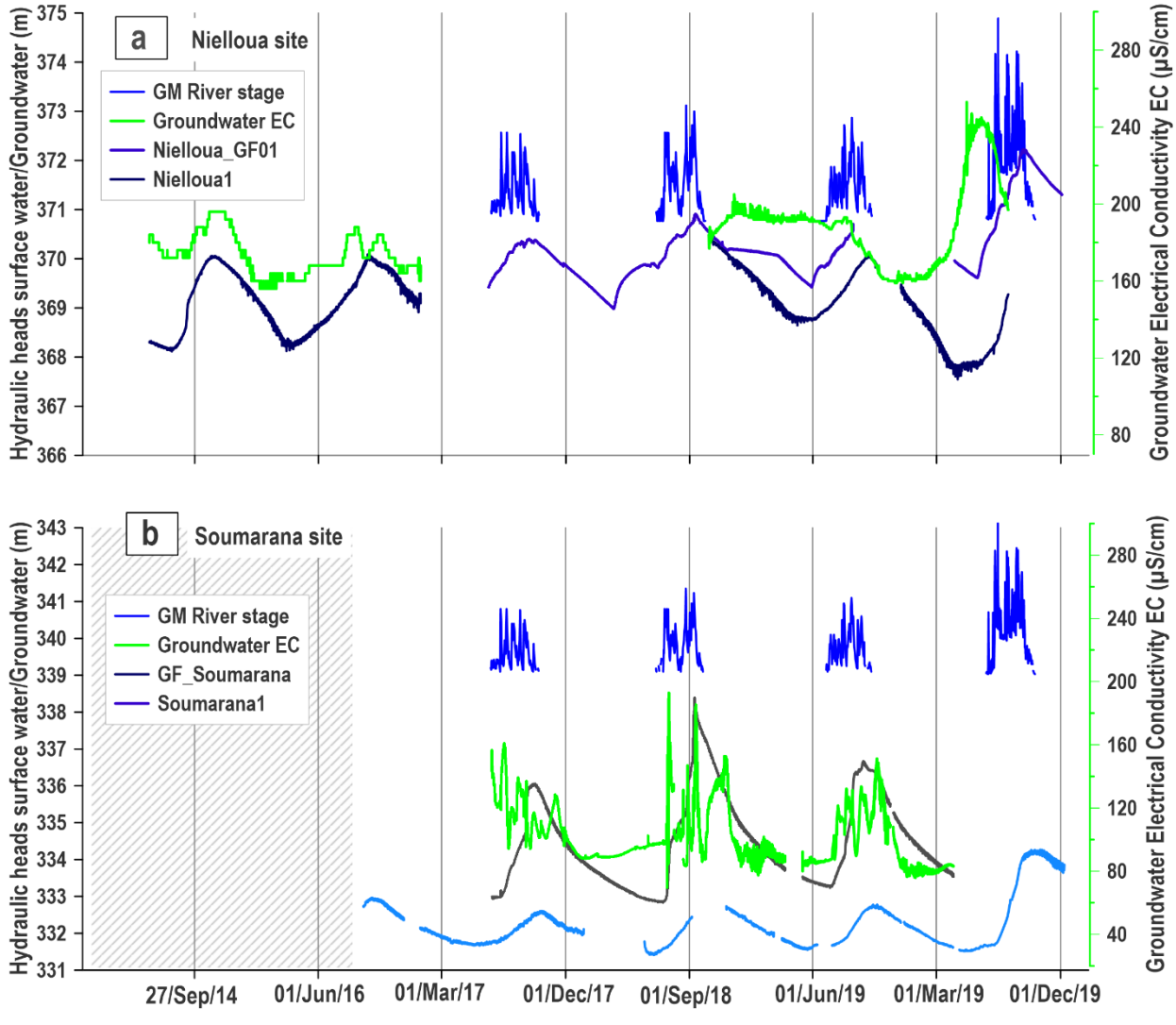

Fig. 6 Seasonal variation in electrical conductivity and hydraulic heads of the alluvial aquifer induced by seasonal river infiltration: **a** Nielloua site**, b** Soumarana site

Groundwater quality for irrigation purposes

Sodium adsorption ratio (SAR)

Calculated SAR values in the alluvial aquifer ranged between 0.7 and 4.9 meq/L whereas, in the aquifer CH, they were between 0.4 and 32.8 meq/L; average values were 2.4 and 9.7 meq/L (Table 4). For a more illustrative assessment of irrigation water quality, groundwater samples for the two aquifers were plotted in the USSLS diagram (USSL 1954), where EC is considered a salinity hazard and SAR is considered an alkalinity hazard (Bian et al. 2018; Zhao et al. 2021). Fig. 7a shows 55% (5/9) and 45% (4/9) of the samples of alluvial aquifer, 50% (7/14) and 7% (1/14) of CH samples, are in the C1-S1, C2-S1 zones respectively. These first two classes are associated with low/medium salinity risk (C1/C2) and low sodium (S1), and therefore, these waters are suitable for irrigation on most soil types with good to excellent quality. For the rest of the CH samples, 7% (1/14) are in the C2-S4 (medium salinity - high sodium hazard) zone, corresponding to water usable for irrigation only for very tolerant plants. 14% (2/14), 7% (1/14) and 14% (2/14) are in the unsafe zone of C3-S1, C3-S2, and C3-S4 (high salinity with low sodium risk, medium sodium risk, and very high sodium risk), respectively. Waters of classes (C3-S1, C3-S2) may be used on coarse-textured soils with good permeability and management measures such as salt filtration, good drainage system, and organic matter increase should be formulated in advance for avoiding possible adverse effects on crops according to the different salt content (Zhao et al. 2021). However, the waters of the C3S4 are inadequate for irrigation, and their use will cause damage to soils and plants.

Percent sodium (%Na)

The %Na value ranges from 22-73% in the alluvial aquifer and 11-97% in the CH, with 43 and 56% for average values, respectively (Table 4). Based on Wilcox's (1955) classification (Table 4), which considers only the %Na, and generally, when its value is > 60%, the water becomes unsuitable for agricultural irrigation. Statistically, 100% (9/9) and 65% (9/14) of shallow alluvial aquifer and CH samples, respectively, waters are good to acceptable for irrigation.

Fig. 7b classifies irrigated water into four categories: good to permissible, permissible to doubtful, doubtful to unsuitable, and unsuitable. All samples of the alluvial aquifer (9/9) and 57% (8/14) of CH samples, respectively, were considered to be good to excellent water for irrigation. Other CH samples fall into the class of good to permissible (2/14, 14%), permissible to doubtful (1/14, 7%), and doubtful to unsuitable (3/14, 21%).

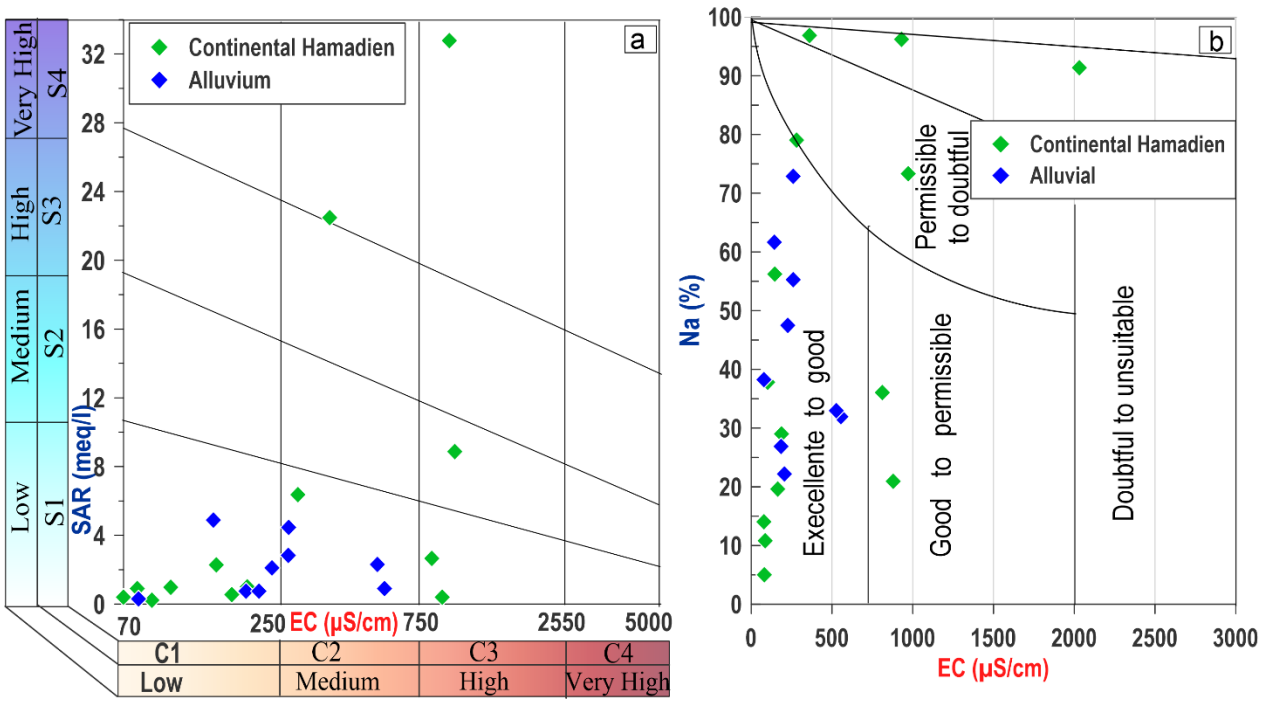

Fig. 7 Suitability of irrigation water for the alluvial and Continental Hamadien aquifers: **a** USSL Diagram, **b** Wilcox Diagram

Residual sodium carbonate (RSC)

The RSC also categorizes the suitability of groundwater for irrigation uses. Calculated values ranged between -0.04-2.56 meq/L in the alluvial aquifer, while in the aquifer CH, they were between -2.24-2.72 meq/L. The average values are -0.82 and 0.86 meq/L (Table 4). Based on Richards's (1954) classification, all alluvial water samples and 11/14 (79%) of CH water samples had an RSC < 2.5 meq/L, indicating that water quality from these sites was suitable for irrigation purposes. Nevertheless, 3/14 (21%) of water samples of CH had an RSC > 2.5 meq/L. A rise in the RSC value beyond the reference level suggests that an increased Na^+ absorption by soil may restrict water and air movement through into soil and then decrease soil permeability which was unsuitable for crop growth and yield (Bian et al. 2018).

Table 4 Water quality classification scheme for irrigation and values found in the study area

Index	Class	Range	Alluvial Aquifer			Continental Hamadien aquifer			References
			Min	Max	Medium	Min	Max	Medium	
CE (µS/cm)	Excellent	< 250	78	555.8	270	78.8	2031	618	Wilcox (1955)
	Good	250 - 750							
	Permissible	750 - 2250							
	Doubtful	2250 - 5000							
	Unsuitable	> 5 000							
SAR (meq/L)	Excellent	< 10	0.7	4.9	2.4	0.4	32.7	9.7	USSL Staff (1954)
	Good	10 - 18							
	Doubtful	18 - 26							
	Unsuitable	> 26							
NA (%)	Excellent	0 - 20	22.2	72.9	43.3	10.8	96.9	55.7	Wilcox (1955)
	Good	20 - 40							
	Permissible	40 - 60							
	Doubtful	60 - 80							
	Unsuitable	> 80							
SRC (meq/L)	Good	< 1.25	- 0.04	2.56	0.82	-2.24	2.72	0.86	Richards (1954)
	Medium	1.25 - 2.5							
	Bad	> 2.5							
	Class II	25 - 75 %							
	Class III	< 75 %	91	146	113	58	160	109	

Discussion

Mechanisms controlling groundwater chemistry

Complex geochemical mechanisms and processes occur during the recharge process or due to the long residence time of water in the saturated zone, including dissolution/precipitation, ion exchange processes, hydrolysis, oxidation, and reduction (Abdou Babaye et al., 2019; Yang et al., 2022). For this study, the diagrams of Gibbs (1970) were used to understand the relationship between the composition of water and these natural processes. As seen in Fig. 8a and b, all groundwater samples are located within the water/rock interaction zone, except two (2) samples from CH. Thus, rock-water interaction, which is an indicator of the chemical alteration of rock-forming minerals, was found to be a major process in groundwater mineralization in the study area.

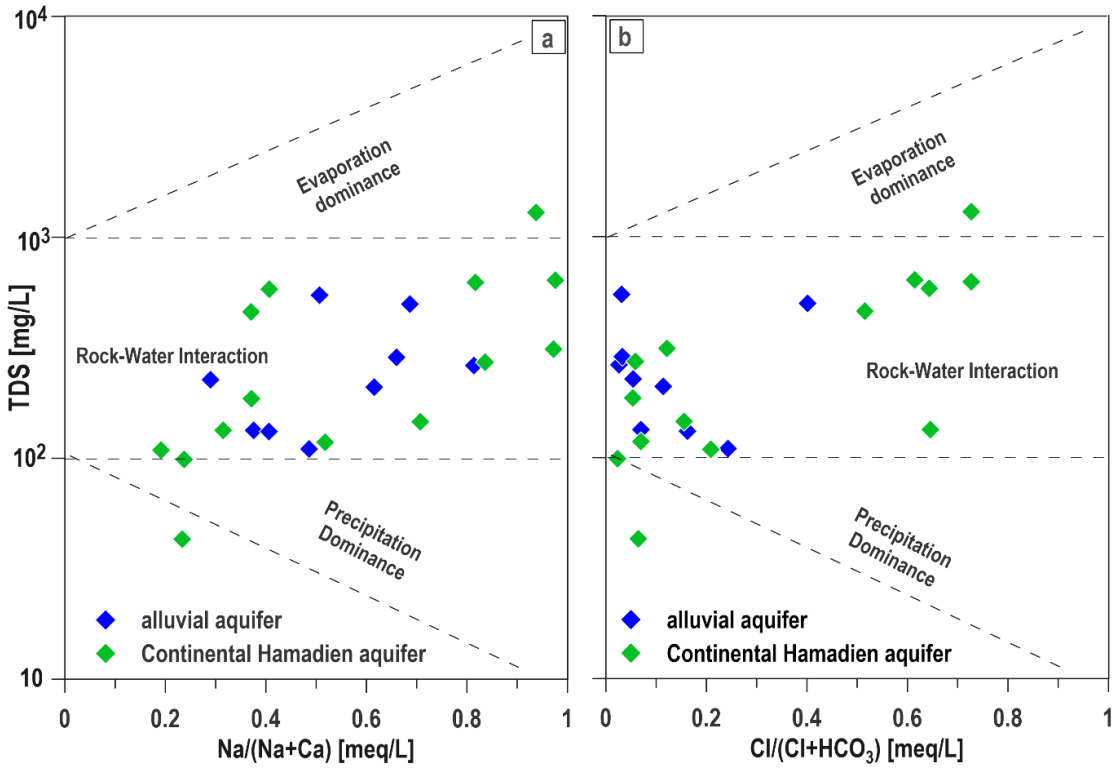

Fig. 8 Gibbs diagrams: **a** TDS versus the weight ratios of Na^+/ (Na^+ + Ca^{2+}), **b** the weight ratios of Cl^-/ (Cl^- + HCO_3^-)

However, in order to further the details of rock-water interaction and determine the origin of each majors element contributing to groundwater mineralization, relationships between (Na^+, K^+) or (Ca^{2+} and Mg^{2+}) with Cl^-, HCO_3^- or SO_4^{2-} are frequently used (Subba Rao et al. 2017; Abdou Babaye et al. 2019; Li et al. 2019).

The geogenic origin of Na^+ and Cl^- ions in groundwater has often been demonstrated by plotting the diagram (Na^+ + K^+) versus Cl^- (Farid et al. 2012; Li et al. 2013; Bahir et al. 2018). For instance, if the dissolution of halite (NaCl) is the important factor controlling the occurrence of Na^+ and Cl^- ions in groundwater, the molar concentrations of Na and Cl should be equal. In this sense, the scatter plot lines up along the line of slope 1:1. However, all samples of alluvial aquifer fell above the halite dissolution line (Fig. 9a), indicating a predominance of (Na^++K^+) over Cl, suggesting that halite dissolution is not the mechanism responsible for the occurrence of Na^+ and Cl^- ions in the alluvial aquifer. Despite this, the saturation indices (SI) of halite with negative values between -6.85 and -9.37 (Table 5) show that the waters are highly unsaturated in this mineral, indicating that these minerals can dissolve into the groundwater if they exist. Furthermore, it has

been reported that high concentrations of Na^+ and Cl^- can be measured when halite is dissolved in groundwater (Panno et al. 2006). In the study area, the concentrations of these ions are relatively low with an average of 28, 11, and 9 mg/L for Na^+, Cl^- and K^+, respectively, and a low correlation ($R^2 = 0.48$) between (Na+K)/Cl is observed. Then, we can assume that the Na^+, K^+, and Cl^- have an atmospheric source with probably an enrichment of Na^+ and K^+, non-conservative during water transfer, which the origin can be associated with the leaching of soil during runoff and in the vadose zone. This argument is supported by the fact that river infiltration is the potential pathway for recharge of the alluvial aquifer, leading to a seasonal increase in both water level and mineral load in the aquifer through increased electrical conductivity (Fig. 6). Therefore, Na^+ ions could have an additional origin related to soil and vadose zone leaching during this recharge process. While in the CH aquifer, there is a strong positive correlation ($R^2 = 82$) between (Na^++k^+) and Cl^-, suggesting that these ions may have common sources, the ($Na^+ + K^+$) vs. Cl^- diagram shows that the scatter plot is on either side of the halite dissolution line, except for F14 sample. SI values strongly negative ranging from -10.64 to -5.44 (Table 5), demonstrate that the CH aquifer is also highly unsaturated for the mineral halite, even though high concentrations of Na^+ (70 to 395 mg/L) and Cl^- (155 to 395 mg/L) were measured in the downstream part of the basin (F12, F13, F14, and F18). However, in the semi-arid environment, the obvious deviation of the samples from the NaCl dissolution line may be caused by cation exchange and/or silicate dissolution (Su et al. 2019; Huang et al. 2022).

The contents of Ca^{2+}, Mg^{2+}, and HCO_3^- in groundwater can often result from carbonate minerals dissolution, such as dolomite ($CaMgCO_3$) and calcite ($CaCO_3$). In this sense, the diagrams ($Ca^{2+} + Mg^{2+}$) and Ca^{2+} versus HCO_3^- can be implemented to explore this mechanism (Li et al. 2018; Abdou Babaye et al. 2019). Theoretically, if the dissolution of dolomite and calcite is responsible for the occurrence of Ca^{2+}, Mg^{2+}, and, HCO_3^- ions in groundwater, the scatter plots relating to the two diagrams must line up according to the slope lines 1:1. However, Fig. **9**b-c shows that there are few samples (3/9, 2/14) and (2/9, 2/14) respectively from the alluvial and CH aquifer fall along the dissolution line of dolomite and calcite. The relative values of SI are negative and range between -7.34 to -1.28, -10.37 to -0.91 for dolomite, and -3.52 to -0.48, -3.98 to -0.01 for calcite, respectively, for alluvial and CH aquifer (Table 5). In the alluvial aquifer, the average concentrations measured of Ca^{2+} and Mg^{2+} are 11 and 3 mg/L, respectively, and a significant correlation between HCO_3^- and Mg^{2+} and Ca^{2+} ($R^2 = 0.67$ and 0.63) have been observed, suggesting

that these ions may have a common source in this aquifer. Contrarily, for the CH samples, both diagrams show an absence of correlation (R^2 = 0.07 and 0.06) between HCO_3^- and Ca^{2+} and Mg^{2+}, suggesting different sources for these ions. Consequently, this suggests that carbonate minerals are not the main source of Ca^{2+}, Mg^{2+}, and HCO_3^- in the waters of the study area. Furthermore, the low average values of 17 and 3 mg/L for Ca^{2+} and Mg^{2+} respectively, may imply depletion of these ions in the lower CH aquifer through cation exchange reactions (Rafique et al. 2015; Olaka et al. 2016; Li et al. 2016; Haji et al. 2018; Su et al. 2019).

In the same boreholes (F12, F13, F14, F18, and F20) with high Na^+ and Cl^-, relatively high concentrations of SO_4^{2-} (50 to 180 mg/L) and F^- (1.12 to 4.3 mg/L) were measured. It has been reported that SO_4^{2-} ions can be associated with gypsum minerals ($CaSO_4$:2H2) dissolution (Farid et al. 2013; Liu et al. 2020). This is demonstrated when the scatter plot of the diagram SO_4^{2-} versus Ca^{2+} line-up along the equilibrium line of slope 1:1. For this study, Fig. **9**d shows that all samples of the alluvial aquifer fell above this line, suggesting insignificant to absent contribution of this mineral in this aquifer. Comparatively, for CH, the scatter plot is on either side of the gypsum dissolution line, except for F14, which is on the line. In addition, the saturation indices calculated with negative values ranging from -3.98 to -2.6 and -5.36 to -1.86 in the alluvial aquifer and the CH, respectively, show that the waters are undersaturated in this mineral.

To discuss the occurrence of high fluoride concentration in groundwater in sedimentary aquifers, especially in arid and semi-arid environments, correlations between F^- and pH, HCO_3^-, can be used (Edmunds and Smedley 2013; Su et al. 2019). Furthermore, when waters are Na-HCO_3 type, such as in our study area, the conditions for fluorine enrichment are conducive and a positive correlation can exist between F^- and HCO_3^-, suggesting that the concentration of F^- increases with both HCO_3^- and pH. Consequently, F^- may be mobilized at the fluoride-bearing minerals (e.g., CaF_2) in response to cation exchange between Na^+ adsorbed on clay minerals with Ca^{2+} and Mg^{2+} in groundwater. As shown under the logarithmic scale, Fig. **9**e and f, a positive correlation can be observed in the study area, therefore suggesting that the concentrations of HCO_3^- and pH favor the release of F^- into groundwater. The same conclusions have been obtained by Haji et al. (2018); Su et al. (2019) and Nordstrom and Smedley (2022).

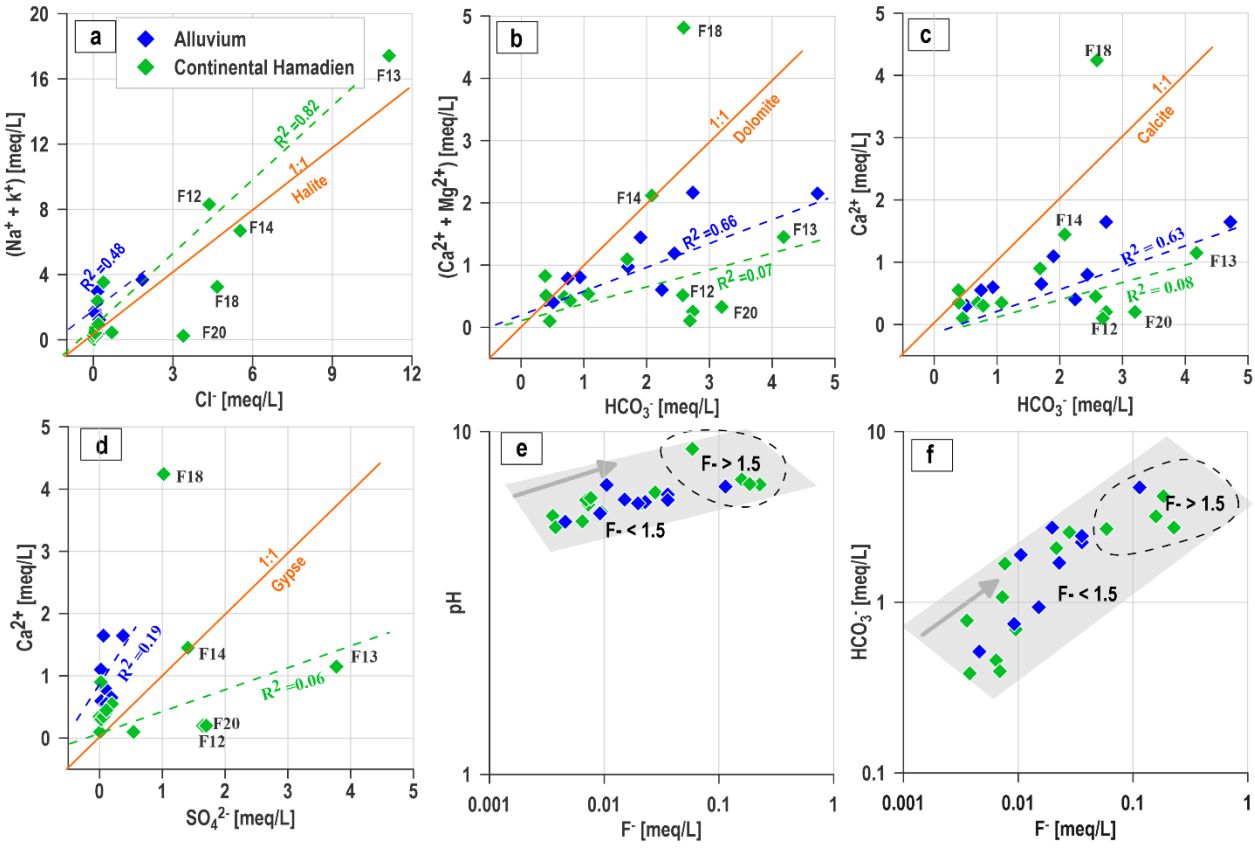

493

494 **Fig. 9** Relationship between hydrochemical compositions: **a** $(Na^+ + K^+)$ vs. Cl^-, **b** $(Ca^{2+} + Mg^{2+})$

495 vs. HCO_3^-, **c** Ca^{2+} vs. HCO_3^-, **d** Ca^{2+} vs. SO_4^{2-}, **e** pH vs. F^-, **f** HCO_3^- vs. F^-

496 Table 5 Saturation indices (SI) of calcite, dolomite, halite, and fluorite

Samples	SI Calcite	SI Dolomite	SI Gypsum	SI Halite	SI Fluorite
Alluvial Aquifer					
P1	-1.47	-3.27	-2.6	-6.85	-2.21
P2	-2.11	-4.49	-3.94	-8.76	-2.76
P3	-0.48	-1.28	-3.37	-8.26	-0.68
P6	-1.72	-3.53	-3.68	-8.62	-2.23
P7	-1.62	-3.36	-3.45	-8.54	-1.95
P10	-1.94	-3.99	-3.18	-8.29	-2.74
P17	-2.78	-5.73	-3.43	-9.37	-3.57
P22	-3.52	-7.34	-3.98	-8.95	-5.04
B4	-0.91	-2.14	-3.86	-8.96	-2.84
Continental Hamadien Aquifer					
B5	-3.98	-10.37	-5.36	-10.64	-4.27
B8	-2.67	-5.46	-4.45	-9.69	-3.67
B9	-2.93	-6.05	-5.23	-10.37	-3.41
B11	-3.57	-7.24	-3.2	-8.39	-4.13

B12	-1.56	-3.5	-2.91	-6.13	-2.41
B13	-0.71	-1.81	-1.96	-5.44	-0.62
B14	-1.64	-3.42	-2.15	-6.14	-2.29
B15	-1.6	-3.67	-3.94	-8.94	-3.22
B16	-3.09	-6.34	-4.21	-9.35	
B18	-0.58	-1.81	-1.86	-6.56	-4.35
B19	-2.46	-4.96	-3.89	-8.42	-3.66
B20	-1.21	-2.42	-2.82	-8.07	-1.34
B21	-1.52	-3.66	-3.58	-8.08	-2.41
B23	-0.01	-0.91	-3.61	-7.54	-2.49

Cation exchange

The importance of cation exchange between Na^+ adsorbed on clay minerals with Ca^{2+} and Mg^{2+} in groundwater can be confirmed when the values of the chloro-alkaline indices (CAI-1 and CAI-2) are negative (Huang et al. 2022). Furthermore, a significant impact of this exchange on the chemical composition of groundwater is evident when the scatter plot of the diagram [$(Na^+ + K^+)$ - Cl^-] versus [$(Ca^{2+} + Mg^{2+})$ - $(HCO_3^- + SO_4^{2-})$] lines up along the line of slope 1:1 (Li et al. 2019; Su et al. 2019). In the study area, the calculated values of CAI-1 and CAI-2 (Fig. 10a) are negative and vary from -28.76 to -1.00 and -0.74 to -0.24 in the alluvial aquifer, and -15.8 to 0.93 and -0.98 to 0.64, respectively in the CH aquifer. Fig. 10b, relating to diagram [$(Na^+ + K^+)$ - Cl^-] versus [$(Ca^{2+} + Mg^{2+})$ - $(HCO_3^- + SO_4^{2-})$], shows that all the points are aligned along the line with a correlation coefficient of $R^2 = 0.90$ and 0.99, respectively from the alluvial and CH aquifer. This confirms cation exchange as the most important hydrochemical process in the study area. Na^+ in the aquifer is exchanged for Mg^{2+} and Ca^{2+} ions in the water.

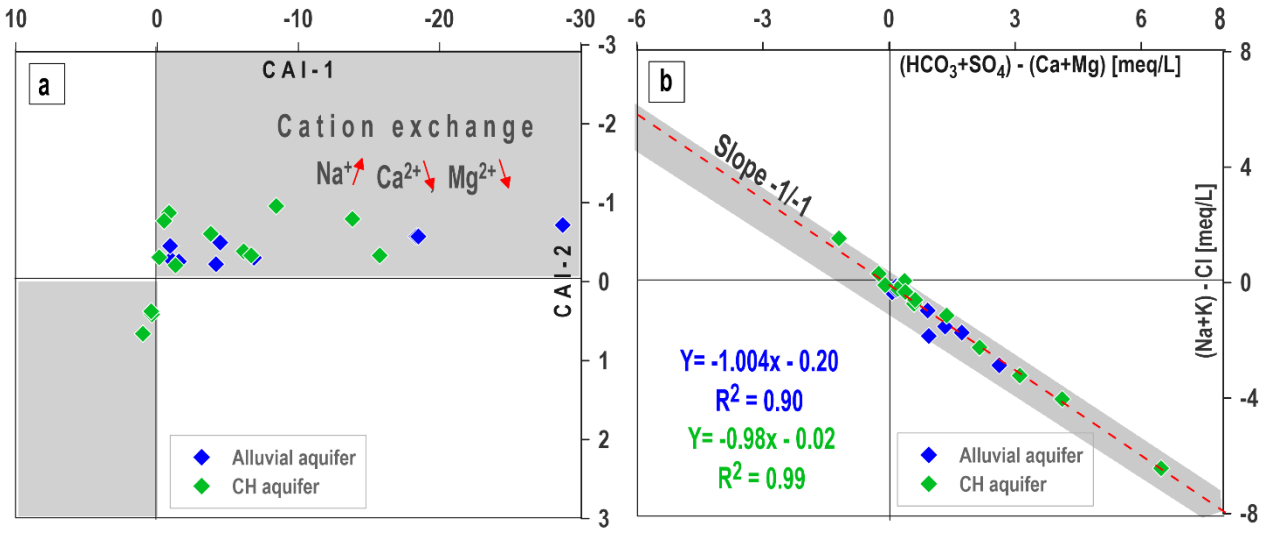

Fig. 10 a Diagram of Chloro-alkaline indices CAI-2 vs. CAI-1 for alluvial and CH aquifer, **b** Diagram (Na + K) – Cl vs. (HCO_3 + SO_4) – (Ca + Mg)

Implications for socio-economic activities and groundwater management

The results of this study have socio-economic implications, including for drinking water supply for the population and irrigation. For example, throughout the study area, it is shown that the groundwater of the alluvial aquifer has excellent potential in terms of quality for the water supply of populations and irrigation. Concerning the aquifer CH, this study shows in the upstream part of the basin, from depths of up to 100 m, the water quality is suitable for all uses. Inversely, in the downstream part, deeper than 60, the water from some boreholes may present a potential danger to human health and are not suitable for irrigation because of the high levels of sodium, chloride, sulfate, and fluorine. In this sense, our study provides important information on the geological and geochemical aspects of finding the favored site and depth of groundwater for development. Better recognition of the spatial distribution of fluoride with depth and identification of the potential contribution of lithology type to fluorine release will require depth-specific sampling and leachate analysis. Thus, our study constitutes the first step toward minimizing the risk to human health linked to water consumption with high fluoride content. This study also contributes to understanding the mechanisms controlling groundwater mineralization and solute mobilization, including fluoride in the study area. In addition, for a better understanding of the geology and the mechanisms that control the hydrochemical characteristics, we built a typical conceptual model of the study area (Fig. 11).

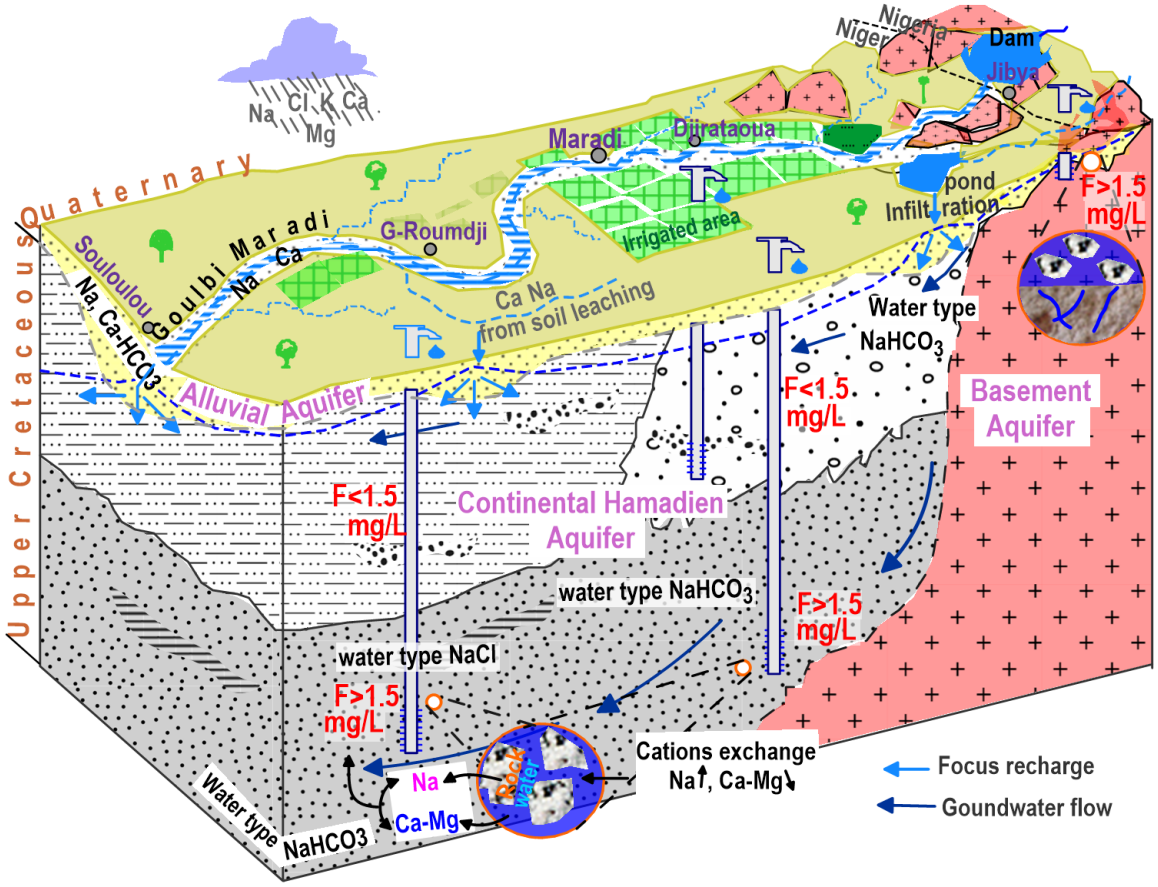

532

533 **Fig. 11** Conceptual model of the geological, hydrological, and geochemical process controlling
534 groundwater mineralization

535 ## Conclusion

536 This research was conducted to understand the hydrochemical characteristics and groundwater
537 quality suitability for irrigation and drinking purposes. Groundwater samples are slightly acidic
538 with 6.3 and 6.49 pH units, and EC presents highly variable values ranging from 78-550 and 66-
539 2030 µS/cm in the alluvial and CH aquifer, respectively. According to the piper diagram, the waters
540 are mainly Na-HCO_3 in the alluvial aquifer and Na-HCO_3 and Na-Cl in the CH aquifer. The
541 suitability of groundwater irrigation was assessed based on the irrigation quality indexes, including
542 SAR, %Na, and RSC. The results show 100 and 65% of samples from the alluvial and CH aquifers
543 respectively, were suitable for irrigation purposes. According to the WHO standards, the major
544 ions (Na^+, K^+, Ca^{2+}, Mg^{2+}, HCO_3^-, SO_4^{2-}, Cl^-, and NO_3^-) concentrations in the two aquifers were
545 generally below tolerance threshold values. While, for the minor elements, one (1) sample (n=9)

from the alluvial aquifer and three (3) samples from CH (n=14) present fluoride concentrations higher than the WHO threshold (1.5 mg/L). The results of these major ions after using Gibbs diagrams, and various bivariate plots indicate the governing hydrogeochemical process is water-rock interaction. This process is controlled by soil leaching during the rainfall and in the unsaturated zone in the alluvial aquifer, while cation exchange is dominant in the CH aquifer.

Acknowledgments The authors wish to acknowledge support from the *GroFutures* (Groundwater Futures in Sub-Saharan Africa - www.grofutures.org) research project funded by the NERC-ESRC-DFID (UK) UPGro program (refs. NE/M008576/1, NE/M008932/1). The authors also acknowledge the participation of the Direction of Hydraulics and Sanitation of Maradi (Ministry of Hydraulics and Sanitation), especially Ms. Issoufa Ibrahim namely *Dingal*, for his assistance in field data collection.

Declarations

Conflict of interest The authors declare that they have no conflict of interest.

References

Abdou Babaye MS, Orban P, Ousmane B, Favreau G, Brouyère S, & Dassargues A (2019) Characterization of recharge mechanisms in a Precambrian basement aquifer in semi-arid south-west Niger. *Hydrogeology Journal*, *27*(2), 475–491. https://doi.org/10.1007/s10040-018-1799-x

Abdou Babaye MS, Hantchi KD, Wagani I, Issoufou Ousmane B, Sandao I (2021) Multi-Criteria Analysis Using Remote Sensing and GIS: Insight into Groundwater Potential of the Fissured Aquifers in the Liptako Socle (Southwestern Niger). *Journal of Water Resource and Protection*, *13*(11), 881–899. https://doi.org/10.4236/JWARP.2021.1311047

Adams EA, Sambu D, Smiley SL (2018) Urban water supply in Sub-Saharan Africa: historical and emerging policies and institutional arrangements. *Https://Doi.Org/10.1080/07900627.2017.1423282*, *35*(2), 240–263. https://doi.org/10.1080/07900627.2017.1423282

Altchenko Y, Villholth K G (2015) Mapping irrigation potential from renewable groundwater in Africa-A quantitative hydrological approach. *Hydrology and Earth System Sciences*, *19*(2),

1055–1067. https://doi.org/10.5194/hess-19-1055-2015

Bahir M, Ouhamdouch S, Carreira PM, Chkir N, Zouari K (2018) Geochemical and isotopic investigation of the aquifer system under semi-arid climate: case of Essaouira basin (Southwestern Morocco). *Carbonates and Evaporites*, *33*(1), 65–77. https://doi.org/10.1007/s13146-016-0323-4

Bian J, Nie S, Wang R, Wan H, Liu C (2018) Hydrochemical characteristics and quality assessment of groundwater for irrigation use in central and eastern Songnen Plain, Northeast China. *Environmental Monitoring and Assessment*, *190*(7), 1–16. https://doi.org/10.1007/S10661-018-6774-4/FIGURES/5

BRGM (1978) *Etudes comparatives du projet du Goulbi de Maradi : Evaluation et gestion des ressources en eaux souterraines du système des alluvions. Rapport BRGM 78 AGE 017*.

Carter R C, Parker A (2009) Climate change, population trends and groundwater in Africa. *Hydrological Sciences Journal*, *54*(4), 676–689. https://doi.org/10.1623/hysj.54.4.676

Chidambaram S, Anandhan P, Prasanna MV, Srinivasamoorthy K, Vasanthavigar M (2013) Major ion chemistry and identification of hydrogeochemical processes controlling groundwater in and around Neyveli Lignite Mines, Tamil Nadu, South India. *Arabian Journal of Geosciences*, *6*(9), 3451–3467. https://doi.org/10.1007/s12517-012-0589-3

Cobbing J (2020) Groundwater and the discourse of shortage in Sub-Saharan Africa. *Hydrogeology Journal*, *28*(4), 1143–1154. https://doi.org/10.1007/S10040-020-02147-5/FIGURES/1

Cobbing J & Hiller B (2019) Waking a sleeping giant: Realizing the potential of groundwater in Sub-Saharan Africa. *World Development*, *122*, 597–613. https://doi.org/10.1016/J.WORLDDEV.2019.06.024

Cuthbert MO, Taylor RG, Favreau G, Todd MC, Shamsudduha M, Villholth KG, … Kukuric N (2019) Observed controls on resilience of groundwater to climate variability in sub-Saharan Africa. *Nature*, *572*(7768), 230–234. https://doi.org/10.1038/s41586-019-1441-7

Davraz A, Özdemir A (2014) Groundwater quality assessment and its suitability in Çeltikçi plain (Burdur/Turkey). *Environmental Earth Sciences 2014 72:4*, *72*(4), 1167–1190.

https://doi.org/10.1007/S12665-013-3036-1https://doi.org/10.1007/S12665-013-3036-1

Descroix L, Mahé G, Lebel T, Favreau G, Galle S, Gautier E., Olivry J-C, Albergel J, Amogu O Cappelaere B, Dessouassi BR, Diedhiou A, Le Breton E, Mamadou I, Sighomnou D (2009) Spatio-temporal variability of hydrological regimes around the boundaries between Sahelian and Sudanian areas of West Africa: A synthesis. *Journal of Hydrology*, *375*(1–2), 90–102. https://doi.org/10.1016/j.jhydrol.2008.12.012

Descroix L, Genthon P, Amogu O, Rajot J-L, Sighomnou D, Vauclin M (2012) Change in Sahelian Rivers hydrograph: The case of recent red floods of the Niger River in the Niamey region. *Global and Planetary Change*, *98–99*, 18–30. https://doi.org/10.1016/j.gloplacha.2012.07.009

Dikouma M. (1990) Fluctuation du niveau marin au Maestrichtien et au Paléocène dans le bassin Intracratonique des Iullemmeden (Ader-Doutchi, Niger). *Thèse Doctorat, Univ. Dijon-Niamey,* 273p.

Durand A, Icole M, Bieda S (1981) Sédiments et climats quaternaires du Sahel central : exemple de la vallée de Maradi (Niger méridional). *UNIV., SERVICE GEOL./NIAMEY/NER*, *VOL. 12*; *N*(January 1981).

Eaton FM (1950) Significance of carbonates in irrigation waters. *Soil Science*, *69*, 123–134.

Edmunds WM, Smedley PL (2013) Fluoride in natural waters. In *Essentials of Medical Geology: Revised Edition* (pp. 311–336). https://doi.org/10.1007/978-94-007-4375-5_13

Elagib NA, Zayed IS, Saad SAG Al, Mahmood MI, Basheer M, Fink AH (2021) Debilitating floods in the Sahel are becoming frequent. *Journal of Hydrology*, *599*, 126362. https://doi.org/10.1016/J.JHYDROL.2021.126362

Farid I, Trabelsi R, Zouari K, Abid K, Ayachi M (2012). Hydrogeochemical processes affecting groundwater in an irrigated land in Central Tunisia. *Environmental Earth Sciences 2012 68:5*, *68*(5), 1215–1231. https://doi.org/10.1007/S12665-012-1788-7

Farid, I., Trabelsi, R., Zouari, K., Abid, K., & Ayachi, M. (2013). Hydrogeochemical processes affecting groundwater in an irrigated land in Central Tunisia. *Environmental Earth Sciences*,

68(5), 1215–1231. https://doi.org/10.1007/s12665-012-1788-7

Favreau G, Cappelaere B, Massuel S, Leblanc M, Boucher M, Boulain N, Leduc C (2009) Land clearing, climate variability, and water resources increase in semiarid southwest Niger: A review. *Water Resources Research*, *45*(7), 1–18. https://doi.org/10.1029/2007WR006785

Favreau G, Nazoumou Y, Leblanc M, Guéro A, Goni IB (2012) Groundwater resources increase in the Iullemmeden Basin, West Africa. *In Climate Change Effects on Groundwater Resources: A Global Synthesis of Findings and Recommendations (Pp. 113-128). CRC Press.*

FIDH (2002) Droit à l'eau potable au Niger Enfants de Tibiri : quand l'eau se transforme en poison Privatisation de la distribution de l'eau : un processus à surveiller.

Fisher RS, Mullican III WF (1997) Hydrochemical Evolution of Sodium-Sulfate and Sodium-Chloride Groundwater Beneath the Northern Chihuahuan Desert, Trans-Pecos, Texas, USA. Hydrogeology Journal, 5(2), 4–16. https://doi.org/10.1007/s100400050102

Gaye CB, Tindimugaya C (2019) Review: Challenges and opportunities for sustainable groundwater management in Africa. Hydrogeology Journal, 27(3), 1099–1110. https://doi.org/10.1007/S10040-018-1892-1/FIGURES/1

Gibbs RJ (1970) Mechanisms controlling world water chemistry. Science, 170(3962), 1088–1090. https://doi.org/10.1126/science.170.3962.1088

Gleeson T, Wang-Erlandsson L, Porkka M, Zipper SC, Jaramillo F, Gerten D, Famiglietti, JS (2020) Illuminating water cycle modifications and Earth system resilience in the Anthropocene. Water Resources Research, 56(4), e2019WR024957. https://doi.org/10.1029/2019WR024957

Goni IB, Taylor RG, Favreau G, Shamsudduha M, Nazoumou Y, Ngounou Ngatcha B (2021) Groundwater recharge from heavy rainfall in the southwestern Lake Chad Basin: evidence from isotopic observations. Hydrological Sciences Journal, 66(8), 1359–1371. https://doi.org/10.1080/02626667.2021.1937630/SUPPL_FILE/THSJ_A_1937630_SM5432.DOCX

Greigert J (1966) Description des formations crétacées et tertiaires du bassin des Iullemmeden.

Rapport BRGM,Orléans, France. 236.

Haji M, Wang D, Li L, Qin, D, Guo Y (2018) Geochemical Evolution of Fluoride and Implication for F− Enrichment in Groundwater: Example from the Bilate River Basin of Southern Main Ethiopian Rift. Water, 10(12), 1799. https://doi.org/10.3390/w10121799

Hutton G & Chase C (2016) The Knowledge Base for Achieving the Sustainable Development Goal Targets on Water Supply, Sanitation and Hygiene. *International Journal of Environmental Research and Public Health 2016, Vol. 13, Page 536*, *13*(6), 536. https://doi.org/10.3390/IJERPH13060536

Huang L, Sun Z, Zhou A, Bi J & Liu Y (2022) Source and enrichment mechanism of fluoride in groundwater of the Hotan Oasis within the Tarim Basin, Northwestern China. *Environmental Pollution*, *300*, 118962. https://doi.org/10.1016/j.envpol.2022.118962

Issa Lélé M & Lamb PJ (2010) Variability of the Intertropical Front (ITF) and Rainfall over the West African Sudan–Sahel Zone. *Journal of Climate*, *23*(14), 3984–4004. https://doi.org/10.1175/2010JCLI3277.1

Issoufou Ousmane B, Nazoumou Y, Favreau G, Abdou Babaye MS, Abdou Mahaman R, Boucher M, Taylor RG, Legchenko A (2021) Caractérisation géophysique des aquifères dans la vallée transfrontalière du Goulbi Maradi (Niger/Nigeria). 12e Colloque GEOFCAN, 05–08. Retrieved from https://hal.inrae.fr/hal-03145437

Issoufou Ousman B, Nazoumou Y, Favreau G, Abdou Babaye MS, Abdou Mahaman R, Boucher M, … Taylor RG (2022) Changes in aquifer properties along a seasonal river channel of the Niger Basin: Identifying groundwater recharge pathways in a dryland environment. *Journal of African Earth Sciences*, 104742. https://doi.org/10.1016/j.jafrearsci.2022.104742

Lapworth DJ, Baran N, Stuart ME & Ward RS (2012) Emerging organic contaminants in groundwater: A review of sources, fate and occurrence. Environmental Pollution, 163, 287–303. https://doi.org/10.1016/J.ENVPOL.2011.12.034

Lapworth DJ, Boving TB, Kreamer DK, Kebede S & Smedley PL (2022) Groundwater quality: Global threats, opportunities and realising the potential of groundwater. Science of The Total

682 Environment, 811, 152471. https://doi.org/10.1016/j.scitotenv.2021.152471

683 Lapworth DJ, Krishan G, MacDonald AM & Rao MS (2017) Groundwater quality in the alluvial
684 aquifer system of northwest India: New evidence of the extent of anthropogenic and geogenic
685 contamination. Science of The Total Environment, 599–600, 1433–1444.
686 https://doi.org/10.1016/J.SCITOTENV.2017.04.223

687 Lebel T & Ali, A (2009) Recent trends in the Central and Western Sahel rainfall regime (1990–
688 2007). Journal of Hydrology, 375(1–2), 52–64. https://doi.org/10.1016/j.jhydrol.2008.11.030

689 Leblanc MJ, Favreau G, Massuel S, Tweed SO, Loireau M & Cappelaere B (2008) Land clearance
690 and hydrological change in the Sahel: SW Niger. *Global and Planetary Change*, *61*(3–4),
691 135–150. https://doi.org/10.1016/J.GLOPLACHA.2007.08.011

692 Li P, He X, Li, Y & Xiang G (2019) Occurrence and Health Implication of Fluoride in Groundwater
693 of Loess Aquifer in the Chinese Loess Plateau: A Case Study of Tongchuan, Northwest China.
694 *Exposure and Health*, *11*(2), 95–107. https://doi.org/10.1007/s12403-018-0278-x

695 Li P, Wu J, Qian, H (2013) Assessment of groundwater quality for irrigation purposes and
696 identification of hydrogeochemical evolution mechanisms in Pengyang County, China.
697 *Environmental Earth Sciences*, *69*(7), 2211–2225. https://doi.org/10.1007/s12665-012-2049-
698 5

699 Li P, Wu J, & Qian, H (2016) Hydrochemical appraisal of groundwater quality for drinking and
700 irrigation purposes and the major influencing factors: a case study in and around Hua County,
701 China. *Arabian Journal of Geosciences*, *9*(1), 15. https://doi.org/10.1007/s12517-015-2059-1

702 Li P, Wu J, Tian R, He S, He X, Xue C & Zhang, K (2018) Geochemistry, Hydraulic Connectivity
703 and Quality Appraisal of Multilayered Groundwater in the Hongdunzi Coal Mine, Northwest
704 China. *Mine Water and the Environment*, *37*(2), 222–237. https://doi.org/10.1007/s10230-
705 017-0507-8

706 Li P, Zhang Y, Yang N, Jing L & Yu, P (2016) Major ion chemistry and quality assessment of
707 groundwater in and around a mountainous tourist town of China. *Exposure and Health*, *8*(2),
708 239–252. https://doi.org/10.1007/s12403-016-0198-6

709 Liu J, Wang M, Gao Z, Chen Q, Wu G, & Li F (2020) Hydrochemical characteristics and water
710 quality assessment of groundwater in the Yishu River basin. Acta Geophysica, 68(3), 877–
711 889. https://doi.org/10.1007/s11600-020-00440-1

712 MacDonald AM, Bonsor HC, Dochartaigh BÉÓ, & Taylor RG (2012) Quantitative maps of
713 groundwater resources in Africa. *Environmental Research Letters*, *7*(2), 024009.
714 https://doi.org/10.1088/1748-9326/7/2/024009

715 Mahe G, Lienou G, Descroix L, Bamba F, Paturel JE, Laraque A, … Khomsi K (2013) The rivers
716 of Africa: witness of climate change and human impact on the environment. Hydrological
717 Processes, 27(15), 2105–2114. https://doi.org/10.1002/HYP.9813

718 Mahe G, Pature, J-E, Servat E, Conway D, & Dezetter A (2005) The impact of land use change on
719 soil water holding capacity and river flow modelling in the Nakambe River, Burkina-Faso.
720 Journal of Hydrology, 300(1–4), 33–43. https://doi.org/10.1016/j.jhydrol.2004.04.028

721 Mechal A, Shube H, Godebo TR, Walraevens K, & Birk S (2022) Application of multi-
722 hydrochemical indices for spatial groundwater quality assessment: Ziway Lake Basin of the
723 Ethiopian Rift Valley. *Environmental Earth Sciences*, *81*(1), 1–22.
724 https://doi.org/10.1007/S12665-021-10135-5/FIGURES/11

725 MHA (2016) *Pragramme sectoriel eau hygiene et assainissement*.

726 Mignon, R (1970) *Étude géologique et prospection du Damagaram Mounio et du Sud Maradi*.

727 Nazoumou Y, Favreau G, Adamou M M, & Maïnassara I (2016) La petite irrigation par les eaux
728 souterraines, une solution durable contre la pauvreté et les crises alimentaires au Niger ?
729 Cahiers Agricultures, 25(1), 15003. https://doi.org/10.1051/cagri/2016005

730 Nordstrom DK, & Smedley PL (2022) Fluoride in groundwater. *Fluoride*.

731 Olaka LA, Wilke FDH, Olago DO, Odada EO, Mulch A, & Musolff A (2016) Groundwater
732 fluoride enrichment in an active rift setting: Central Kenya Rift case study. Science of The
733 Total Environment, 545–546, 641–653. https://doi.org/10.1016/j.scitotenv.2015.11.161

734 OMS (2011) Guidelines for drinking-water quality. *Switzerland Geneva*, undefined-564.

735 Onipe T, Edokpayi JN, & Odiyo JO (2020) A review on the potential sources and health
736 implications of fluoride in groundwater of Sub-Saharan Africa.
737 Https://Doi.Org/10.1080/10934529.2020.1770516, 55(9), 1078–1093.
738 https://doi.org/10.1080/10934529.2020.1770516

739 OSS (2008) Système aquifère d'Iullemeden (Mali, Niger, Nigeria): gestion concertée des
740 ressources en eau partagées d'un aquifère transfrontalier sahélien. *OSS*, (Rapport technique).

741 Panno S V, Hackley K C, Hwang H H, Greenberg S E, Krapac I G, Landsberger S & O'Kelly D J
742 (2006) Characterization and Identification of Na-Cl Sources in Ground Water. *Ground Water*,
743 *44*(2), 176–187. https://doi.org/10.1111/j.1745-6584.2005.00127.x

744 Parkhurst DL, & Appelo CAJ (2013) Description of input and examples for PHREEQC version 3:
745 a computer program for speciation, batch-reaction, one-dimensional transport, and inverse
746 geochemical calculations. *Techniques and Methods*. https://doi.org/10.3133/TM6A43

747 Piper A M (1944) A graphic procedure in the geochemical interpretation of water-analyses. *Eos,*
748 *Transactions American Geophysical Union*, *25*(6), 914–928.
749 https://doi.org/10.1029/TR025I006P00914

750 Rafique T, Naseem S, Ozsvath D, Hussain R, Bhanger MI, & Usmani TH (2015) Geochemical
751 controls of high fluoride groundwater in Umarkot Sub-District, Thar Desert, Pakistan. Science
752 of The Total Environment, 530–531, 271–278.
753 https://doi.org/10.1016/j.scitotenv.2015.05.038

754 Ramesh K, & Elango L (2012) Groundwater quality and its suitability for domestic and agricultural
755 use in Tondiar river basin, Tamil Nadu, India. *Environmental Monitoring and Assessment*,
756 *184*(6), 3887–3899. https://doi.org/10.1007/s10661-011-2231-3

757 Richards L A (1954) Diagnosis and Improvement of Saline and Alkali Soils. In *Soil Science* (Vol.
758 78).

759 Schoeller H (1965) Qualitative evaluation of groundwa-ter resource. In *Methods and techniques of*
760 *groundwater investigations and development. UNESCO Water Resources Series* (pp. 44–52).

761 Su H, Wang J, & Liu J. (2019) Geochemical factors controlling the occurrence of high-fluoride

groundwater in the western region of the Ordos basin, northwestern China. *Environmental Pollution*, *252*, 1154–1162. https://doi.org/10.1016/j.envpol.2019.06.046

Subba Rao N, Marghade D, Dinakar A, Chandana I, Sunitha B, Ravindra B & Balaji T (2017) Geochemical characteristics and controlling factors of chemical composition of groundwater in a part of Guntur district, Andhra Pradesh, India. *Environmental Earth Sciences*, *76*(21), 747. https://doi.org/10.1007/s12665-017-7093-8

Taylor RG, Aureli A, Allen DA, Banks D, Villholth KG and Stigter T (2022) Groundwater, Aquifers and Climate Change (Chapter 7). In The United Nations World Water Development Report 2022: Groundwater: Making the invisible visible. UNESCO (Paris), pp. 101-114.

Taylor, RG, Scanlon B, Döll P, Rodell M, Van Beek R, Wada Y, … Treidel H (2013) Ground water and climate change. *Nature Climate Change*, *3*(4), 322–329. https://doi.org/10.1038/nclimate1744

Tschakert P, Sagoe R, Ofori-Darko G & Codjoe S N (2010) Floods in the Sahel: an analysis of anomalies, memory, and anticipatory learning. *Climatic Change 2009 103:3*, *103*(3), 471–502. https://doi.org/10.1007/S10584-009-9776-Y

UN (2019) Revision of World Population Prospects. Retrieved January 21, 2021, from https://population.un.org/wpp/

USSL (1954) Diagnosis and Improvement of Saline and Alkaline Soils. *Soil Science Society of America Journal*, *18*(3), 348. https://doi.org/10.2136/sssaj1954.03615995001800030032x

WHO/UNICEF (2015) *Joint Water Supply, Sanitation Monitoring Programme, & World Health Organization. Progress on sanitation and drinking water: 2015 update and MDG assessment.*

WHO (2011) *Guidelines for drinking-water quality. World Health Organization. 216*, *303–3*.

WHO (2019) *Drinking-water*. Retrieved from https://www.who.int/news-room/fact-sheets/detail/drinking-water.

Wilcox L V (1948) The Quality of Water for Irrigation Use, US Department of Agriculture, Technical Bulletin No. 962, Washington, D.C.,.

Wilcox L V (1955) *Classification and use of irrigation waters*. 969.

Xu Y, Seward P, Gaye C, Lin L & Olago D O (2019) Preface: Groundwater in Sub-Saharan Africa. *Hydrogeology Journal*, *27*(3), 815–822. https://doi.org/10.1007/S10040-019-01977-2/FIGURES/1

Yang N, Su C, Liu W & Zhao L (2022) Occurrences and mechanisms of strontium-rich groundwater in Xinglong County, northern China: insight from hydrogeological and hydrogeochemical evidence. *Hydrogeology Journal*, 1–15. https://doi.org/10.1007/s10040-022-02533-1

Zaman M, Shahid SA & Heng L (2018) Irrigation Water Quality. *Guideline for Salinity Assessment, Mitigation and Adaptation Using Nuclear and Related Techniques*, 113–131. https://doi.org/10.1007/978-3-319-96190-3_5

Zhao X, Guo H, Wang Y, Wang G, Wang H, Zang X & Zhu J (2021) Groundwater hydrogeochemical characteristics and quality suitability assessment for irrigation and drinking purposes in an agricultural region of the North China plain. *Environmental Earth Sciences*, *80*(4), 1–22. https://doi.org/10.1007/S12665-021-09432-W/FIGURES/5